広島大学学位論文

Analyses of zebrafish Ddx46 function in the tissue and organ formation

組織・器官形成におけるゼブラフィッシュ Ddx46 の機能解析

2015 年

広島大学大学院理学研究科
生物科学専攻
平林　諒

目　次

１．主論文

Analyses of zebrafish Ddx46 function in the tissue and organ formation.
(組織・器官形成におけるゼブラフィッシュ Ddx46 の機能解析)
平林　諒

２．公表論文

Ddx46 is required for multi-lineage differentiation of hematopoietic stem cells in zebrafish.
Ryo hirabayashi, Shunya Hozumi, Shin-ichi Higashijima, and Yutaka Kikuchi.
Stem cells and Development 2013 sep. 22 (18) pp. 2532-2542

主論文

Analyses of zebrafish Ddx46 function in the tissue and organ formation

- Contents –

I. General introduction ..... p. 5
Figures ..... p. 9
References ..... p. 15

II. Analyses of Ddx46 function in zebrafish hematopoiesis including hematopoietic stem cells development. ..... p. 20
Abstract ..... p. 20
Introduction ..... p. 21
Materials & Methods ..... p. 23
Results ..... p. 26
Discussion ..... p. 30
Figures & Tables ..... p. 32
References ..... p. 51

III. General conclusion ..... p. 56
References ..... p. 59
Acknowledgement ..... p. 62

I. General Introduction

Precursor mRNA (pre-mRNA) splicing is one of the critical steps for gene expression in metazoan. In the process of gene transcription, RNA polymerase II produced pre-mRNA, and it has two types of sequence region called exon (protein coding region) and intron (non-coding region) [1-4]. Exon and intron exist alternately on DNA or RNA sequence. Translating mature mRNA that multiple exons combined produces a protein. Pre-mRNA direct translation cannot make correct protein, therefore each process of the removal introns and the combining exons, is required for corrects protein producing. In pre-mRNA splicing process, mRNA is modified and removed intron by the spliceosome. Spliceosome is large RNA-protein complex composed of five small nuclear ribonucleoprotein particles (snRNPs) and some other proteins. There are two types of spliceosomes involved in pre-mRNA splicing. The spliceosome, which consists of U1, U2, U4, U5, and U6 snRNPs, is involved in the general splicing catalysis [1-4]. Many previous studies revealed the mechanism of pre-mRNA splicing by spliceosome, but it has not been fully elucidated.

We previously isolated the *morendo (mor)* mutant during the mutagenesis with N-ethyl-Nnitrosourea chemical mutagen (Fig. I-1). Analysis of the *mor* mutant responsible gene identified that it has a point mutation on *DEAD-box polypeptide 46* (*Ddx46*). In the *mor* mutant, a serine at the position amino acid protein 942 in the C-terminal domain of the Ddx46 is replaced isoleucine and This I942S allele line is named mor^{ha4} mutant (Fig. I-2A, B).

Ddx46 is the member of the DEAD-box RNA helicase protein family. The DEAD/H-box RNA helicase is a large protein group in Super family 2 (SF2) helicase family and its helicase domain is highly conserved from bacteria to humans [5-8]. DEAD-box protein has specific sequence D-E-A-D, which are responsible for the name of DEAD-box protein and DEAD-box protein is also called DExD/H-box protein as boarder name. The DExD/H-box helicases share nine conserved motifs; motifs Q, I, II, and VI are required for NTP/ATP binding and catalyze its hydrolysis [5-8]. Prp5 that is yeast orthologue Ddx46 is has been studied and is necessary along with ATP hydrolysis, for stable

association of U2 snRNP with pre-mRNA and prespliceosome formation in *Schizosaccharomyces cerevisiae* and *Schizosaccharomyces pombe* [9-12]. Besides Prp5, yeast other DExD/H-box protein, Sub2, Prp28, Brr2, Prp2, Prp16, Prp22, and Prp43, are revealed the function in specific step of the splicing and RNP remodeling [2-4]. In addition, human DDX46 has been shown to play roles in pre-mRNA splicing *in vitro* before or during prespliceosome assembly [13]. However Ddx46 function *in vivo* had not been fully elucidated. Hence we used mor^{ha4} mutants to elucidate Ddx46 function *in vivo*.

First, we tried the phenotypic analysis in mor^{ha4} mutants to find the effects of Ddx46. Then we found digestive organs and brain were defects in mor^{ha4} mutants (Fig. I-1). We next validated whether defects in mor^{ha4} mutants are caused by *Ddx46-I942S* point mutation. The result showed point mutation on *Ddx46* is responsible for the defects in mor^{ha4} mutant, but this point mutated Ddx46 state had not been clearly. We therefore decided to use another allele *Ddx46* mutants called $Ddx46^{hi2137/hi2137}$. This *Ddx46* allele *hi2137* was isolated during an insertional mutagenesis screening (Fig. I-2C, D) [14]. The phenotype of $Ddx46^{hi2137/hi2137}$ mutant is similar to mor^{ha4} mutant, and shows more tightly defects.

Our next experiment was gene expression analysis in digestive organs and brain. Molecular markers, which had been considered necessary for the development of digestive organs and brain, were reduced in $Ddx46^{hi2137/hi2137}$ mutants.

Because yeast Prp5 and human DDX46 are known to be involved in pre-mRNA splicing, we tested whether the *Ddx46* mutant had defects in this process. For the analyses of pre-mRNA splicing in the $Ddx46^{hi2137/hi2137}$ mutants, we examined the splicing status of four genes (*deltaA* (*dla*) [15, 16] and *hairy-related 6* (*her6*) [17] in the brain, and *fatty acid binding protein 10a* (*fabp10a*) [18] and *pancreas specific transcription factor, 1a* (*ptf1a*) [19] in the digestive organs) by performing an RT-PCR analysis that is often used to detect unspliced forms of mRNAs [20-22]. The analysis showed that the unspliced mRNAs were retained in the $Ddx46^{hi2137/hi2137}$ mutants at 3 or 4 days postfertilization (dpf) (Figure. I-3), suggesting that the pre-mRNA splicing process is defective in this mutant, as observed in yeast.

To test whether the effect on pre-mRNA splicing is restricted to a subset of genes or general, we further examined the pre-mRNA splicing of various

genes, including housekeeping genes. The results suggest that the effect of pre-mRNA splicing may be specific to a certain set of genes in the *Ddx46*$^{hi2137/hi2137}$ mutants.

We previous validated to define the spatiotemporal expression of *Ddx46* in developing embryos and larvae; we performed whole-mount *in situ* hybridization. We found that *Ddx46* has a maternally supplied transcript that was expressed ubiquitously during early somitogenesis. Its expression became restricted to the head region by 24 hours postfertilization (hpf). By 2 dpf, *Ddx46* was expressed in the head, retina, digestive organs, and pectoral fin bud, and at 4 dpf, its expression was even more confined to the retinae, telencephalon, midbrain, midbrain-hindbrain boundary, branchial arches, esophagus, liver, pancreas, and intestinal bulb. Transverse section data revealed the presence of the *Ddx46* transcript in pancreatic exocrine cells but not in pancreatic endocrine cells. Further, we found that *Ddx46* transcripts were not present in the somite after 4 dpf. These *Ddx46* expression patterns were consistent with nearly all aspects of the *mor*^{ha4} and *Ddx46*$^{hi2137/2137}$ mutant phenotype.

Our previous analysis of Ddx46 function in *Ddx46* mutants (*mor*^{ha4} and *Ddx46*$^{hi2137/2137}$) revealed that Ddx46 is also involved in pre-RNA splicing *in vivo* and the region of defects in *Ddx46* mutants corresponded with *Ddx46* expression pattern. We therefore expected that the region of *Ddx46* expressed has defects in *Ddx46* mutants and found the novel expression in hematopoietic tissue.

In vertebrate hematopoiesis is highly conserved and there are two important steps such as primitive and definitive hematopoiesis [23-25]. Primitive hematopoiesis is the temporary hematopoiesis to rapid supply blood cells in early development. While no blood cells are produced from HSCs in primitive hematopoiesis, hemangioblast produces blood cells parallel with blood vessel formation (Fig. I-4A-C) [23-26]. Hematopoietic stem cells (HSCs) are differentiated from AGM in definitive hematopoiesis (Fig. I-4D and Fig. I-5A). HSCs move to the caudal hematopoietic tissue (CHT) and produce all lineage blood cells (Fig. I-4E, F and Fig. I-5B, C). The hematopoiesis in CHT is also temporary and HSCs in CHT is move again to kidney and thymus as adult hematopoietic organs (Fig. I-5D-F). These processes (temporary primitive hematopoiesis, HSCs are differentiated from AGM, and move adult hematopoietic tissue or organs through the temporary

hematopoietic place such as CHT) are conserved in other vertebrates [23, 24].

The zebrafish has emerged as an important model system for the investigation of vertebrate development and other complex biological processes, including human disease [27, 28]. Some report said the pre-mRNA splicing defects had been shown in hematological disorder [29-32]. However, no study reported Ddx46 function in hematopoiesis.

We therefore expected Ddx46 is involved in hematopoiesis and analyzed *Ddx46*$^{hi2137/2137}$ mutants to reveal the novel Ddx46 function in hematopoiesis.

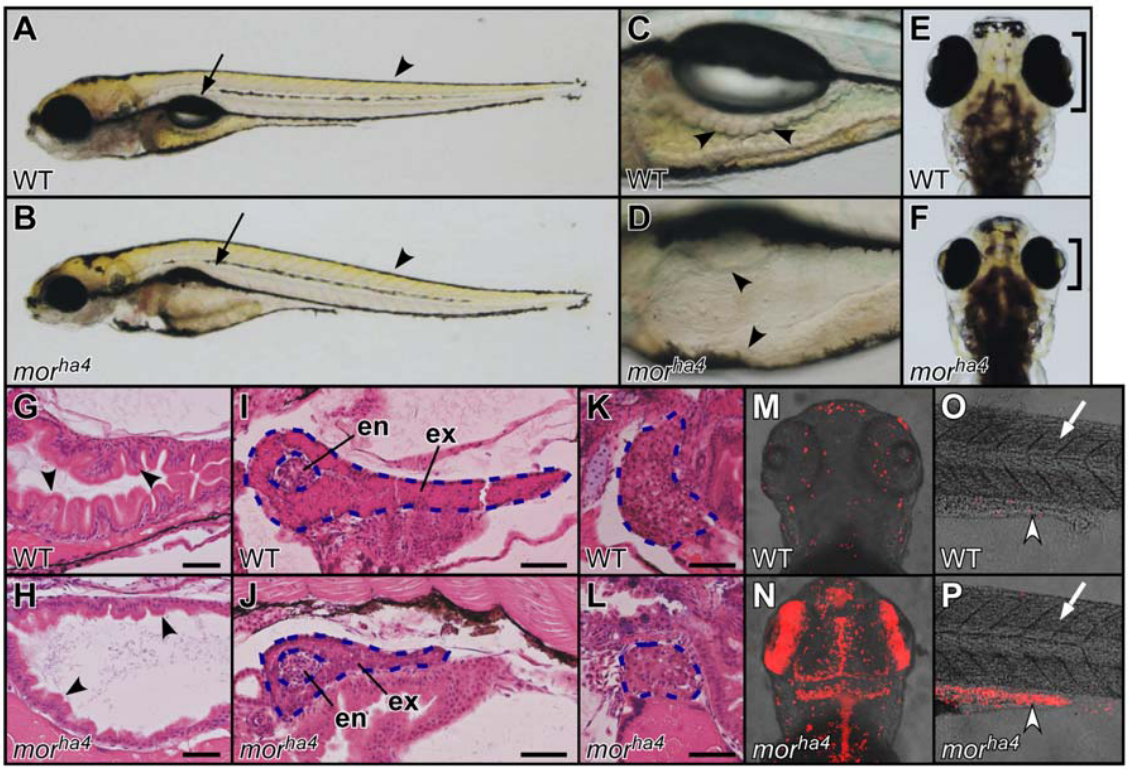

FIG. I-1. Phenotype of the *mor*^{ha4} mutant.

(A–F) Lateral (A–D) and dorsal (E, F) views of live WT and *mor*^{ha4} larvae at 5.5 dpf. The swim bladder failed to inflate (arrows in A, B), the intestine lacked folds (arrowheads in C, D), and the retinae were reduced in size (brackets in E, F) in the *mor*^{ha4} mutant. Conversely, somite formation in the *mor*^{ha4} mutant appeared normal (arrowheads in A, B). (G–L) Sagittal sections of 5.5-dpf larvae stained with hematoxylin and eosin. The intestine lacked folds and was thin walled (arrowheads in G, H), and the exocrine pancreas (blue dotted lines in I, J) and liver (blue dotted lines in K, L) were small in the *mor*^{ha4} mutant. In contrast, the endocrine pancreas (blue dotted lines in I, J) in WT larvae was indistinguishable from that in *mor*^{ha4} larvae. Scale bars, 50 mm. (M–P) Dorsal views, anterior to the top (M, N). Lateral views, anterior to the left (O, P). Apoptotic cells were detected using the TUNEL method. An increase in apoptotic cells was evident in the brain, retinae, and posterior intestine of the *mor*^{ha4} larvae (white arrowheads in O, P) compared to WT larvae, but not in the *mor*^{ha4} somite (white arrows in O, P). en, endocrine pancreas; ex, exocrine pancreas.

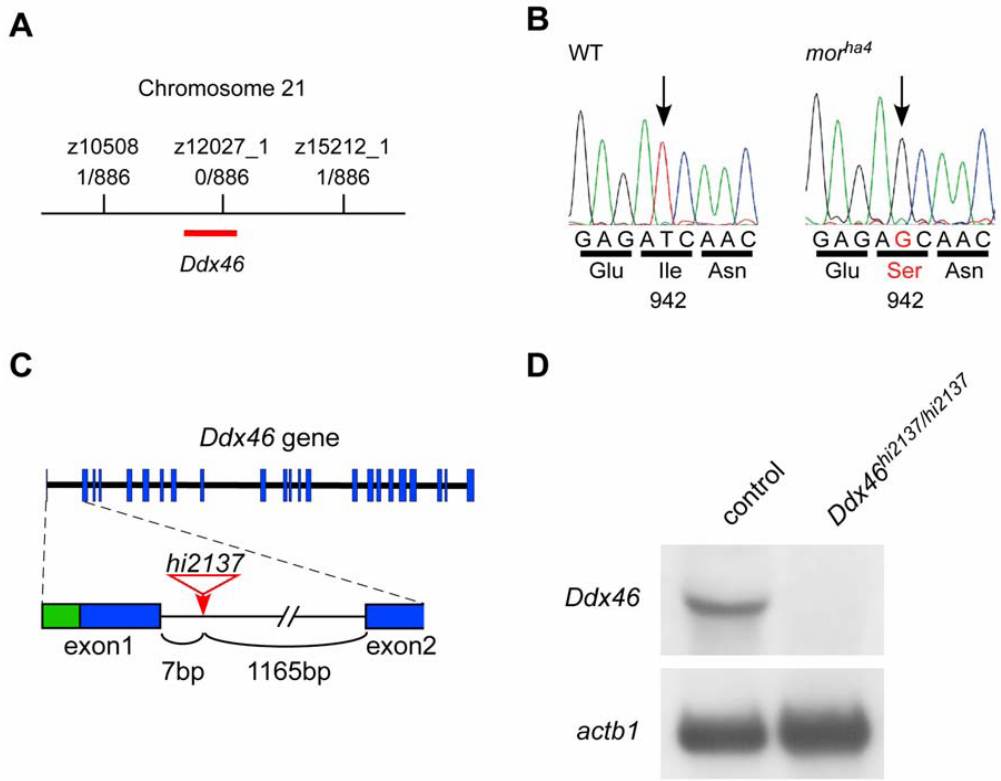

FIG. I-2. Identification of the *mor* gene and analysis of the *hi2137* allele.

(A) Meiotic and physical map schematic of the *mor* locus on chromosome 21. The number of recombinants and larvae genotyped is shown for each microsatellite marker. (B) Sequencing cDNA from WT and mor^{ha4} larvae revealed a nucleotide exchange from T to G, which resulted in an Ile-to-Ser transition at amino acid 942 in the mor^{ha4} mutant. (C) Genomic structure of the *Ddx46* gene showing the viral insertion site in the *hi2137* allele (red). Exons are boxes, with coding and non-coding sequences in blue and green, respectively. The viral insertion (red arrow) occurs in the first intron between exons 1 and 2. (D) Northern blot analysis of $Ddx46^{hi2137/hi2137}$ mutants and control larvae at 3.5 dpf. No Ddx46 transcript was found in the $Ddx46^{hi2137/hi2137}$ mutants, whereas the level of *actb1* transcript in the mutants was the same as that in control larvae. Control larvae were sibling WT or $Ddx46^{hi2137/+}$ larvae and had normal phenotypes.

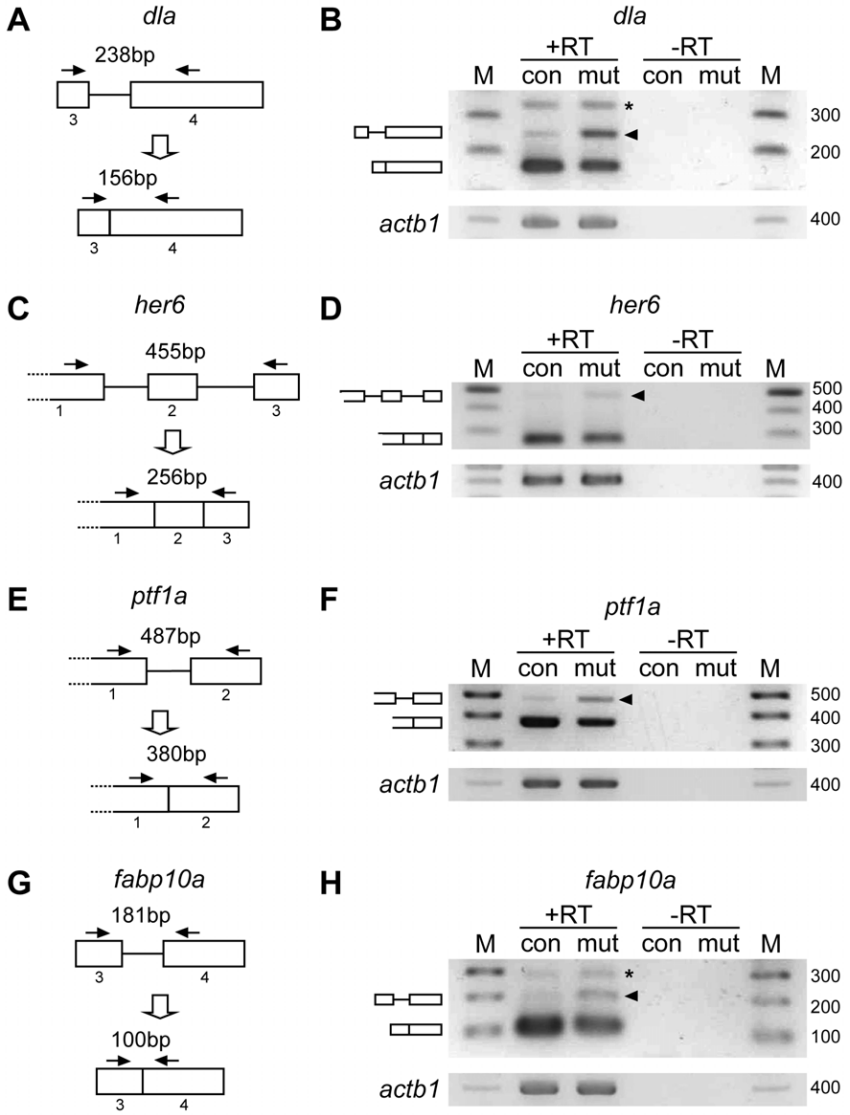

FIG. I-3. Ddx46 deficiency affects pre-mRNA splicing in the digestive organs and brain.

(A–H) Scheme of the *dla*, *her6*, *ptf1a*, and *fabp10a* pre-mRNA regions analyzed for splicing (boxes, exons; lines, introns; arrows, primers) (A, C, E, G). The splicing status of *dla*, *her6*, *ptf1a*, and *fabp10a* pre-mRNA was monitored using RT-PCR with the primers indicated in scheme A, C, E, and G, respectively. Unspliced *dla*, *her6*, *ptf1a*, and *fabp10a* mRNAs were retained in the *Ddx46*$^{hi2137/hi2137}$ mutant (mut) larvae compared to the control (con) larvae (arrowheads in B, D, F, H). Unspliced and spliced PCR products were verified by sequencing. +RT refers to the validation reaction itself, and 2RT represents the respective control reaction without reverse transcriptase. *actb1* is a loading control by using primers designed in the exon 6. M, DNA size markers (sizes in bp); the asterisks point to nonspecific PCR products. Control larvae were sibling WT or *Ddx46*$^{hi2137/+}$ larvae and had normal phenotypes.

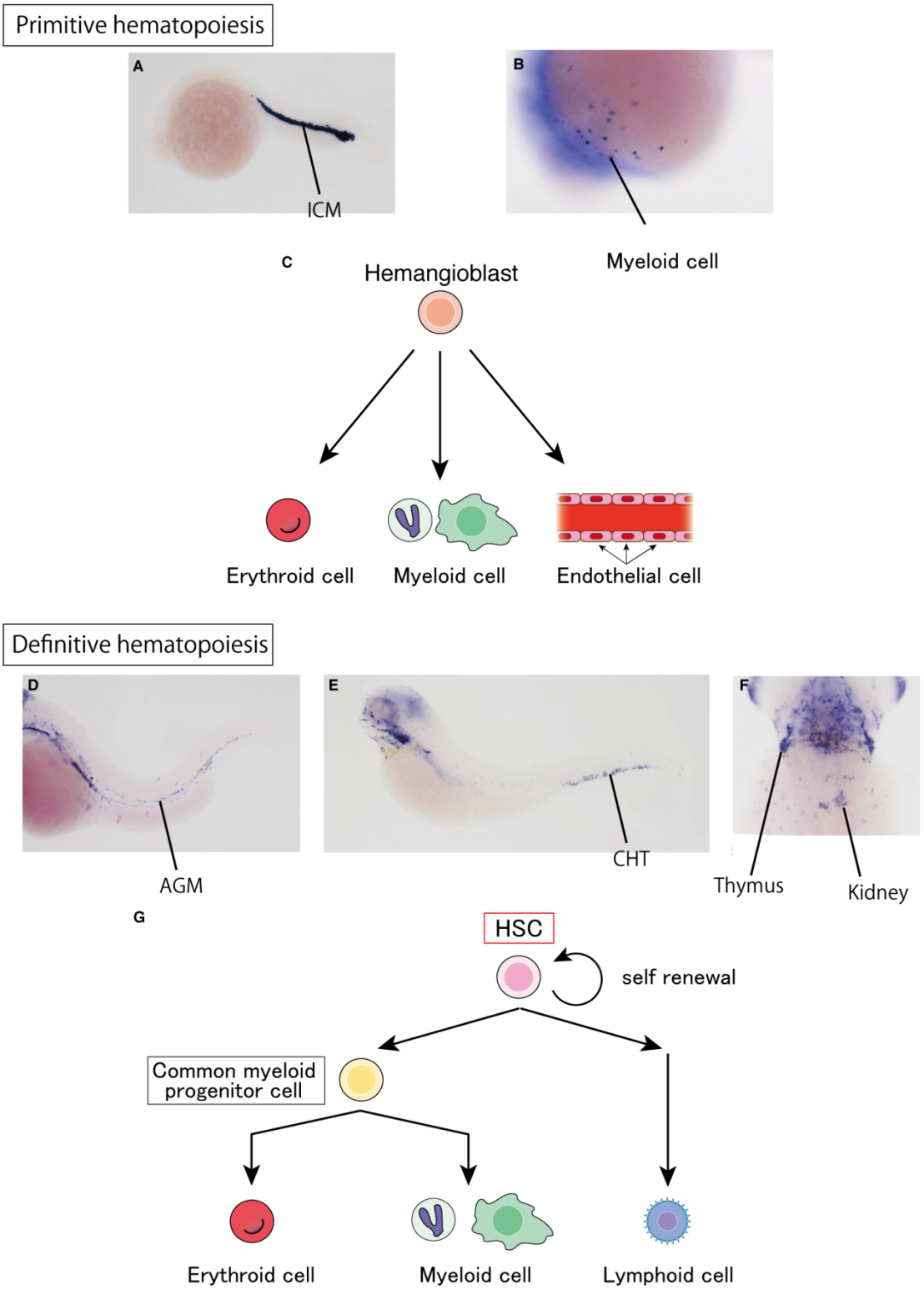
Primitive hematopoiesis
A
ICM
B
Myeloid cell
C
Hemangioblast
Erythroid cell
Myeloid cell
Endothelial cell
Definitive hematopoiesis
D
AGM
E
CHT
F
Thymus
Kidney
G
HSC
self renewal
Common myeloid progenitor cell
Erythroid cell
Myeloid cell
Lymphoid cell

FIG. I-4. Primitive and definitive hematopoiesis in zebrafish.

(A–G) They are the gene expression of hematopoietic markers and the model of hematopoiesis; (A–C) primitive hematopoiesis and (D–G) definitive hematopoiesis. (A, B, D, E) All are lateral views, anterior to the left. (E) It is dorsal views, anterior to the upside. (A-B) The expression of *hbbe3* and *mpx* at 22 hpf. (D-F) The expressions of *cmyb* at 2, 3 and 4 dpf. (A) The primitive hematopoietic marker expression region is ICM that produces blood cells and endothelial cells from hemangioblast. (B) Myeloid cells exist at front side in primitive hematopoiesis. (C) The model primitive hematopoiesis. (D-F) Definitive hematopoietic marker *cmyb* expressed in AGM, CHT, thymus and kidney. (G) The model of blood cell differentiation after definitive hematopoiesis. All blood cell lineages are differentiated from HSC. Both erythroid cell and myeloid cell have same progenitor cell called common myeloid progenitor cell. HSC, hematopoietic stem cell; ICM, intermediate cell mass; AGM, aorta-gonad-mesonephros; CHT, caudal hematopoietic tissue; hpf, hours postfertilization; dpf, days postfertilization.

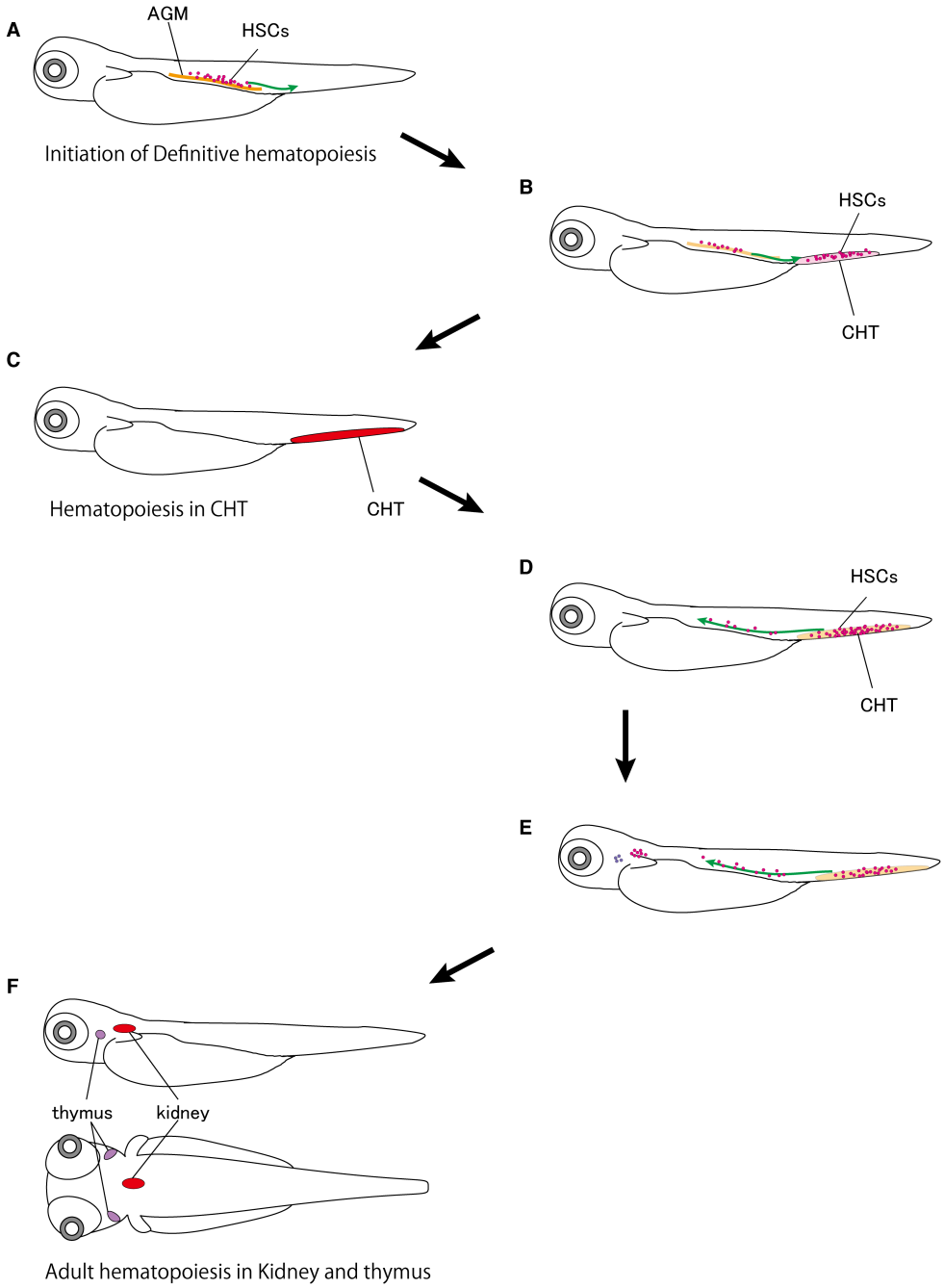

FIG. I-5. HSCs movement during definitive hematopoiesis to adult hematopoiesis in zebrafish.

(A, B) HSCs are differentiated from hemogenic endothelium in AGM and move CHT. (C) HSCs in CHT produce blood cells temporarily. (D–E) Through the course of the development, HSCs move again to adult hematopoietic region. (F) A hematopoiesis in CHT is finally disappeared. Both kidney and thymus are adult hematopoietic organs in zebrafish.

References

1. Staley JP, Guthrie C (1998) Mechanical devices of the spliceosome: motors, clocks, springs, and things. Cell 92: 315–326.

2. Brow DA (2002) Allosteric cascade of spliceosome activation. Annu Rev Genet 36: 333–360.

3. Smith DJ, Query CC, Konarska MM (2008) "Nought may endure but mutability": spliceosome dynamics and the regulation of splicing. Mol Cell 30:657–666.

4. Wahl MC, Will CL, Lu¨hrmann R (2009) The spliceosome: design principles of a dynamic RNP machine. Cell 136: 701–718.

5. Silverman E, Edwalds-Gilbert G, Lin RJ (2003) DExD/H-box proteins and their partners: helping RNA helicases unwind. Gene 312: 1–16.

6. Rocak S, Linder P (2004) DEAD-box proteins: the driving forces behind RNA metabolism. Nat Rev Mol Cell Biol 5: 232–241.

7. Bleichert F, Baserga S (2007) The long unwinding road of RNA helicases. Mol Cell 27:339–352.

8. Jankowsky E (2011) RNA helicases at work: binding and rearranging. Trends Biochem Sci 36: 19–29.

9. Ruby SW, Chang TH, Abelson J (1993) Four yeast spliceosomal proteins (PRP5, PRP9, PRP11, and PRP21) interact to promote U2 snRNP binding to premRNA. Genes Dev 7: 1909–1925.

10. Xu Y, Newnham C, Kameoka S, Huang T, Konarska M, et al. (2004) Prp5 bridges U1 and U2 snRNPs and enables stable U2 snRNP association with intron RNA. EMBO J 23: 376–385.

11. Xu YZ, Query CC (2007) Competition between the ATPase Prp5 and branch region-U2 snRNA pairing modulates the fidelity of spliceosome assembly. Mol Cell 28: 838–849.

12. Kosowski TR, HR Keys, TK Quan and SW Ruby. (2009). DExD/H-box Prp5 protein is in the spliceosome during most of the splicing cycle. RNA 15:1345-62.

13. Will C, Urlaub H, Achsel T, Gentzel M, Wilm M, et al. (2002) Characterization of novel SF3b and 17S U2 snRNP proteins, including a human Prp5p homologue and an SF3b DEAD-box protein. EMBO J 21: 4978–4988.

14. Amsterdam A, Nissen R, Sun Z, Swindell E, Farrington S, et al. (2004) Identification of 315 genes essential for early zebrafish development. Proc Natl Acad Sci U S A 101: 12792–12797.

15. Haddon C, Smithers L, Schneider-Maunoury S, Coche T, Henrique D, et al.(1998) Multiple delta genes and lateral inhibition in zebrafish primary neurogenesis. Development 125: 359–370.

16. Smithers L, Haddon C, Jiang YJ, Lewis J (2000) Sequence and embryonic expression of deltaC in the zebrafish. Mech Dev 90: 119–123.

17. Pasini A, Henrique D, Wilkinson D (2001) The zebrafish Hairy/Enhancer-ofsplit- related gene her6 is segmentally expressed during the early development of hindbrain and somites. Mech Dev 100: 317–321.

18. Her G, Chiang C, Chen W, Wu J (2003) In vivo studies of liver-type fatty acid binding protein (L-FABP) gene expression in liver of transgenic zebrafish (Danio rerio). FEBS Lett 538: 125–133.

19. Zecchin E, Mavropoulos A, Devos N, Filippi A, Tiso N, et al. (2004) Evolutionary conserved role of ptf1a in the specification of exocrine pancreatic fates. Dev Biol 268: 174–184.

20. Ko¨nig H, Matter N, Bader R, Thiele W, Mu¨ ller F (2007) Splicing segregation: the minor spliceosome acts outside the nucleus and controls cell proliferation. Cell 131: 718–729.

21. Rı´os Y, Melmed S, Lin S, Liu NA (2011) Zebrafish usp39 mutation leads to rb1 mRNA splicing defect and pituitary lineage expansion. PLoS Genet 7:e1001271. 36. Ro¨ sel TD, Hung LH, Medenbach J, Donde K, Starke S, et al. (2011) RNA-Seqanalysis in mutant zebrafish reveals role of U1C protein in alternative splicing regulation. EMBO J 30: 1965–1976.

22. Ro¨ sel TD, Hung LH, Medenbach J, Donde K, Starke S, et al. (2011) RNA-Seqanalysis in mutant zebrafish reveals role of U1C protein in alternative splicing regulation. EMBO J 30: 1965–1976.

23. Orkin SH and LI Zon. (2008). Hematopoiesis: an evolving paradigm for stem cell biology. Cell 132:631-44.

24. Paik EJ and LI Zon. (2010). Hematopoietic development in the zebrafish. Int J Dev Biol 54:1127-37.

25. Cumano A and I Godin. (2007). Ontogeny of the hematopoietic system. Annu Rev Immunol 25:745-85.

26. Medvinsky A, S Rybtsov and S Taoudi. (2011). Embryonic origin of the adult hematopoietic system: advances and questions. Development 138:1017-31.

27. Lieschke GJ, Currie PD (2007) Animal models of human disease: zebrafish swim into view. Nat Rev Genet 8: 353–367.

28. Skromne I, Prince VE (2008) Current perspectives in zebrafish reverse genetics: moving forward. Dev Dyn 237: 861–882.

29. Yoshida K, M Sanada, Y Shiraishi, D Nowak, Y Nagata, R Yamamoto, Y Sato, A Sato-Otsubo, A Kon, M Nagasaki, G Chalkidis, Y Suzuki, M Shiosaka, R Kawahata, T Yamaguchi, M Otsu, N Obara, M Sakata-Yanagimoto, K Ishiyama, H Mori, F Nolte, WK Hofmann, S Miyawaki, S Sugano, C Haferlach, HP Koeffler, LY Shih, T Haferlach, S Chiba, H Nakauchi, S Miyano and S Ogawa. (2011). Frequent pathway mutations of splicing machinery in myelodysplasia. Nature 478:64-9.

30. Hahn CN and HS Scott. (2012). Spliceosome mutations in hematopoietic malignancies. Nat Genet 44:9-10.

31. Quesada V, L Conde, N Villamor, GR Ordóñez, P Jares, L Bassaganyas, AJ Ramsay, S Beà, M Pinyol, A Martínez-Trillos, M López-Guerra, D Colomer, A Navarro, T Baumann, M Aymerich, M Rozman, J Delgado, E Giné, JM Hernández, M González-Díaz, DA Puente, G Velasco, JM Freije, JM Tubío, R Royo, JL Gelpí, M Orozco, DG Pisano, J Zamora, M Vázquez, A Valencia, H Himmelbauer, M Bayés, S Heath, M Gut, I Gut, X Estivill, A López-Guillermo, XS Puente, E Campo and C López-Otín. (2012). Exome sequencing identifies recurrent mutations of the splicing factor SF3B1 gene in chronic lymphocytic leukemia. Nat Genet 44:47-52.

32. Graubert TA, D Shen, L Ding, T Okeyo-Owuor, CL Lunn, J Shao, K Krysiak, CC Harris, DC Koboldt, DE Larson, MD McLellan, DJ Dooling, RM Abbott, RS Fulton, H Schmidt, J Kalicki-Veizer, M O'Laughlin, M Grillot, J Baty, S Heath, JL Frater, T Nasim, DC Link, MH Tomasson, P Westervelt, JF DiPersio, ER Mardis, TJ Ley, RK Wilson and MJ Walter. (2012). Recurrent mutations in the U2AF1 splicing factor in myelodysplastic syndromes. Nat Genet 44:53-7.

II. Analyses of Ddx46 function in zebrafish hematopoiesis including hematopoietic stem cells development

Abstract

Balanced and precisely controlled processes between self-renewal and differentiation of HSCs into all blood lineages are critical for vertebrate definitive hematopoiesis. However, the molecular mechanisms underlying the maintenance and differentiation of HSCs have not been fully elucidated. Here, we show that zebrafish *Ddx46*, encoding a DEAD-box RNA helicase, is expressed in HSCs of the CHT. The number of HSCs expressing the molecular markers *cmyb* or *T-cell acute lymphocytic leukemia 1* (*tal1*) was markedly reduced in *Ddx46* mutants. However, massive cell death of HSCs was not detected, and proliferation of HSCs was normal in the CHT of the mutants at 48 hpf. We found that myelopoiesis occurred, but erythropoiesis and lymphopoiesis were suppressed, in *Ddx46* mutants. Consistent with these results, the expression of *spi1*, encoding a regulator of myeloid development, was maintained, but the expression of *gata1a*, encoding a regulator of erythrocyte development, was downregulated in the mutants. Taken together, our results provide the first genetic evidence that zebrafish Ddx46 is required for the multi-lineage differentiation of HSCs during development, through the regulation of specific gene expressions.

Introduction

It has been well noted that the processes involved in vertebrate hematopoiesis during development consist of two evolutionarily conserved steps: primitive hematopoiesis followed by definitive blood formation [1–3]. In the definitive hematopoiesis stage, all blood lineages arise from self-renewing HSCs, and hematopoiesis derived from HSCs persists for the lifetime of vertebrates [1–3]. In recent years, zebrafish has been used as an excellent vertebrate system for studying hematopoiesis during development [4, 5]. In the definitive hematopoietic wave of zebrafish embryos, HSCs originate from the ventral wall of the dorsal aorta (VDA) in the AGM region [2–4]. These HSCs then migrate to an intermediate hematopoietic site, the CHT, and then further toward the kidney or the thymus, which are definitive hematopoietic or lymphopoietic organs, respectively, in adult zebrafish [2–4]. Several lines of genetic evidence have revealed that at least two transcription factors, *cmyb* and *Runt-related transcription factor 1* (*Runx1*), have been implicated in the initiation, maintenance, and/or differentiation of HSCs during vertebrate development [5–14]. Studies on murine and human hematopoietic cell lines have shown that the *cmyb* proto-oncogene, encoding a transcription factor, is expressed mainly in HSCs, and its expression is downregulated in differentiated hematopoietic cells [5]. In addition, studies in a mouse model have suggested that *cmyb* plays critical roles in HSC maintenance and differentiation during development [6–8]. Consistent with observations that have been made in mice, zebrafish *cmyb* mutants have defects in definitive hematopoiesis, suggesting that *cmyb* function is evolutionarily conserved [9, 10]. On the other hand, *runx1* is expressed in the VDA of mouse and zebrafish embryos [11, 12], and analyses of Runx1 knockout mice and zebrafish mutants have revealed that Runx1 is required for the emergence of HSCs at the beginning of definitive hematopoiesis [5, 13, 14]. In contrast to these 2 factors, analyses of mutant animals have shown that the *T-cell acute lymphocytic leukemia 1* (*Tal1*; also known as *Scl*) gene, encoding a basic-helix-loop-helix transcription factor, is required for both hematopoietic and endothelial development [1, 2, 5]. Further, in vitro experiments using mouse embryonic stem cells revealed that Tal1 plays

critical roles in both hemogenic endothelium population generation and definitive hematopoietic specification [15]. Further, the function of *Tal1* is upstream of *Runx1* in definitive hematopoiesis [15]. The molecular mechanisms underlying the initiation, maintenance, and differentiation of HSCs, however, remain to be elucidated. DExD/H-box proteins belong to an evolutionarily conserved family of RNA helicases [16, 17]. The DExD/H-box RNA helicases are known to function in all aspects of RNA metabolism such as pre-mRNA splicing, rRNA biogenesis, and transcription by using the energy derived from ATP hydrolysis [16, 17]. By genetic screening using zebrafish, two DExD/H-box genes, Ddx18 and Dhx8, have been identified thus far as novel genes that are essential for hematopoiesis [18, 19]. A recent study has reported that Ddx18 is required for primitive hematopoiesis through the regulation of p53-dependent G1 cell-cycle arrest [18]. Moreover, a sequence variation in human DDX18, which acts as a dominant- negative, was identified in samples from patients with acute myeloid leukemia [18]. A more recent report showed that a mutation in Dhx8, a zebrafish orthologue of the yeast splicing factor Prp22, led to defects in cell division, pre-mRNA splicing, and primitive hematopoiesis [19]. However, the requirement and function of the DExD/H-box RNA helicases in hematopoiesis are still largely unknown in vertebrates. Our study has previous elucidated that Ddx46, a member of the DEAD-box RNA helicase family, is required for the development of digestive organs and the brain, possibly by regulating pre-mRNA splicing [20]. Here, we show zebrafish *Ddx46* expression in HSCs during development. Moreover, we investigated the phenotype of a zebrafish *Ddx46* mutant in definitive hematopoiesis, and we report the function of Ddx46 in HSC differentiation during development.

Materials & Methods

Ethics statement

All animal experiments were conducted according to relevant national and international guidelines "Act on Welfare and Management of Animals" (Ministry of Environment of Japan). Ethics approval from the Hiroshima University Animal Research Committee (HuARC) was not sought since this law does not mandate protection of fish.

Maintenance and staging of zebrafish

Adult zebrafish and zebrafish embryos were maintained as described by Westerfield [21]. Embryos were incubated in 1/3 Ringer's solution (39mM NaCl, 0.97mM KCl, 1.8mM CaCl2, and 1.7mM HEPES, pH 7.2) at 28.5° C and staging was performed as described by Kimmel *et al.* [22]. The *Ddx46* allele *hi2137* was isolated during an insertional mutagenesis screening (http://web.mit.edu/hopkins/group11.html) [23], and the *Ddx46*$^{hi2137/+}$ fish was obtained from the Zebrafish International Resource Center. Generation of Tg(*tal1*:*EGFP*) fish Approximately 8 kb of the 5' upstream sequence of *tal1* [24, 25] was polymerase chain reaction (PCR)-amplified from zebrafish genomic DNA. The amplified *tal1* promoter, *EGFP*, and *SV40 poly(A)* were placed in the pT2KXIG Δ in vector that has *Tol2* transposable elements [26]. Microinjection of *Tol2*-based plasmid DNA was performed as described previously [27].

Whole-mount *in situ* hybridization, immunehistochemistry, detection of cell death, and genotyping

Single and double whole-mount *in situ* hybridizations were performed as described previously [21, 27], and riboprobes were prepared according to previously published methods. To detect apoptotic cells, we performed TUNEL staining using an *in situ* Cell Death Detection Kit (Roche Diagnostics) according to the manufacturer's instructions. In addition to TUNEL staining, we performed acridine orange staining for apoptosis detection. Live larvae were stained with 10 mg/mL of acridine orange [acridine orange hemi (zinc chloride) salt; Sigma] in 1/3 Ringer's solution for

15min, and then washed thrice with 1/3 Ringer's solution for 5 min each. To evaluate cell proliferation, we performed whole-mount immunohistochemistry as described previously [21]. Mouse monoclonal anti-proliferating cell nuclear antigen (PCNA) antibody (Sigma) and Alexa Fluor® 594 goat anti-mouse IgG antibody (Invitrogen, Life Technologies Corp.) were used as primary and secondary antibodies, respectively. The stained embryos/larvae were embedded in 0.5% low melting temperature agarose in 1/3 Ringer's solution and imaged on an Olympus FV1000-D confocal microscope. Following the whole-mount *in situ* hybridization, TUNEL staining, or immunohistochemical staining, *Ddx46*$^{hi2137/hi2137}$ mutants were confirmed by genotyping as described previously [20].

mRNA and DNA injections

The pCS2 + vector carrying a cDNA fragment encoding Ddx46, EGFP, or *Tol2*-transposase [27] was used in this study. Capped mRNA was synthesized using an SP6 mMESSAGE mMACHINE (Ambion, Life Technologies Corp.). For the overexpression experiments, *Ddx46* or *EGFP* mRNA (320 pg each) was injected at the one-cell stage. For phenotypic rescue experiments of *GATA-binding protein 1a* (*gata1a*) [28], *Tol2*-mediated transgenesis was performed as described previously [29]. At the one-cell stage, 12.5 pg of pT8.1gata1 Δ 3-EGFP (pT-EGFP), which contained the promoter region of *gata1a* and *EGFP*, or pT8.1gata1 Δ 3-FLgata1 (pT-FLgata1), which contained the promoter region of *gata1a* and FLAG-tagged *gata1a*, was co-injected with 25 pg of *Tol2*-transposase mRNA [29].

Quantitative real-time PCR

Total RNA was prepared using TRIzol (Invitrogen, Life Technologies Corp.) from the tails of 50 combined samples of the 3 days dpf control (con) or *Ddx46*$^{hi2137/hi2137}$ mutant larvae that were identified morphologically or molecularly. Con larvae were sibling wild-type (WT) or *Ddx46*$^{hi2137/+}$ larvae, and they had normal phenotypes. DNase-treated RNA (750 ng) was reverse transcribed with random 9-mer priming and reverse transcriptase XL (AMV) (TaKaRa). Quantitative PCR (qPCR) for *spi1* (also known as *pu.1*) [30] and *gata1a* was performed in triplicate using the Thermal Cycler Dice® Real Time System, SYBR® *Premix* Ex Taq™ (TaKaRa Bio, Inc.), and total RNA

prepared as previous elucidated, according to the manufacturer's instructions. The amplified signals were confirmed to be a single band by gel electrophoresis, and they were normalized to the signals of zebrafish 18S rRNA. The primers used were as follows: *gata1a*, 5'-GGCTAGTTCACTC-CATGATC-3' and 5'-CTCAGAGCTGGAGTAGAAAG-3'; *spi1*, 5'-ATGTGGA-GTCCAGCCATTTC-3' and 5'-TTGTGAGG- GTAACACACCGA-3'; 18S rRNA, 5'-CCGCTAGAGGTGAAATTCTTG-3' and 5'-CAGCTTTGCAACCATACTC-C-3'.

Reverse transcription-PCR analysis of splicing

Reverse transcription (RT)-PCR was performed using total RNA prepared as previous elucidated to monitor the splicing of *spi1*, *gata1a*, and *cmyb*. The primer pairs and detailed PCR conditions used to amplify each of these genes are listed in the Tables S1 and S2.

Results

Ddx46$^{hi2137/hi2137}$ mutants have defects in definitive hematopoiesis but not primitive hematopoiesis

We have previous elucidated that *Ddx46*$^{hi2137/hi2137}$ mutants have defects in the formation of digestive organs and the brain [20]. In the course of the phenotypic analyses of *Ddx46*$^{hi2137/hi2137}$ mutants, we also found that the expression of hematopoietic markers was downregulated in the mutants. At 22 hpf, the expression of the primitive hematopoietic markers *tal1*, *LIM domain only 2* (*lmo2*) [31], *gata1a*, *hemoglobin beta embryonic-3* (*hbbe3*) [32], and *myeloid- specific peroxidase* (*mpx*) [33] was normal in *Ddx46*$^{hi2137/hi2137}$ mutants (Fig. II-1A–J). On the other hand, the expression of the HSC markers *tal1*, *runx1*, and *cmyb* was markedly reduced in *Ddx46*$^{hi2137/hi2137}$ mutants at 3 dpf (Fig. II-1K–P). These results indicate that definitive hematopoiesis, but not primitive hematopoiesis, was defective in the mutants.

To confirm that the loss of *Ddx46* is responsible for the observed phenotype in definitive hematopoiesis, we compared the expression pattern of *Ddx46* with that of *cmyb* in the CHT. Ubiquitous expression of *Ddx46* in the AGM and CHT was observed at 2 dpf (Fig. II-2A), and dotted expression of *Ddx46* was found in the CHT at 3 dpf (Fig. II-2B, C). At 4 dpf, the dotted expression pattern of *Ddx46* in the CHT was similar to the expression pattern of *cmyb* (Fig. II-2D, E). Moreover, the expression of both genes overlapped in the CHT, as analyzed by double whole-mount *in situ* staining (Fig. II-2F), indicating that *Ddx46* is expressed in the HSCs at 4 dpf. We next examined whether rescue was achieved by the overexpression of *Ddx46* mRNA. The expressions of *cmyb* and *tal1* were rescued in the *Ddx46* mRNA-injected *Ddx46*$^{hi2137/hi2137}$ mutants (*cmyb*, 19 of 21 *Ddx46* mRNA-injected mutants were rescued; *tal1*, 19 of 22 *Ddx46* mRNA-injected mutants were rescued; Fig. II-3C, F), compared with that in the *EGFP* mRNA-injected *Ddx46*$^{hi2137/hi2137}$ mutants (*cmyb*, 0 of 26 *EGFP* mRNA-injected mutants were rescued; *tal1*, 0 of 21 *EGFP* mRNA-injected mutants were rescued; Fig. II-3B, E) at 3 dpf. The overlapping expression of *Ddx46* and *cmyb* in the CHT and data from the rescue experiments clearly indicate that the defects in definitive hematopoiesis in *Ddx46*$^{hi2137/hi2137}$ mutants are caused by the loss of *Ddx46*.

Expression of molecular markers for HSCs decreases in *Ddx46*$^{hi2137/hi2137}$ mutants without cell death or cell growth defects

Previous studies on zebrafish and mouse development showed that HSCs originate from the VDA in the AGM, and they then migrate to the CHT [2–4]. To determine when definitive hematopoiesis was affected in *Ddx46*$^{hi2137/hi2137}$ larvae, we next counted the number of *cmyb*-expressing HSCs at 36 hpf, 48 hpf, and 3 dpf. The number of *cmyb* expressing HSCs was indistinguishable between *Ddx46*$^{hi2137/+}$ (Fig. II-4A, G) and *Ddx46*$^{hi2137/hi2137}$ larvae (Fig. II-4B, G) at 36 hpf. In contrast, the number of *cmyb*-expressing HSCs in the CHT, but not in the AGM, at 48 hpf and in both the AGM and CHT at 3 dpf was lower in *Ddx46*$^{hi2137/hi2137}$ larvae (Fig. II-4D, F, G) than in *Ddx46*$^{hi2137/+}$ larvae (Fig. II-4C, E, G). To exclude the possibility that the formation of the VDA is affected in *Ddx46*$^{hi2137/hi2137}$ mutants, we examined the expressions of *runx1* and *kinase insert domain receptor like* (*kdrl*; also known as *flk1*) [31], an endothelial marker, in the VDA at 48 hpf. The expression of these genes was normal in the mutants at this stage (Fig. II-5). These results suggest that the emergence of HSCs from the VDA is normal, but the expression of *cmyb*, a molecular marker for HSCs is not maintained in *Ddx46*$^{hi2137/hi2137}$ mutants.

Possible explanations for the reduction of *tal1*-, *runx1*-, or *cmyb*-expressing HSCs in *Ddx46*$^{hi2137/hi2137}$ larvae are the upregulation of cell death or the downregulation of cell proliferation. We first examined cell death of HSCs in the AGM and CHT from 36 hpf to 4 dpf by TUNEL analysis and acridine orange staining because massive apoptosis was observed in digestive organs and the brain of *Ddx46*$^{hi2137/hi2137}$ larvae at 3 dpf, and these larvae cannot survive beyond 5 dpf [20]. From 24 hpf to 4 dpf, increased cell death was not detected in the AGM or CHT of the *Ddx46*$^{hi2137/hi2137}$ larvae (Fig. II-6 and Fig. II-7, and data not shown) compared with that in the *Ddx46*$^{hi2137/+}$ larvae. We next examined cell proliferation using the *Ddx46*^{hi2137}; Tg(*tal1*:*EGFP*) transgenic line. Confocal images of the anti-PCNA immunostaining and EGFP fluorescence indicated that the proliferation of *tal1*-expressing HSCs was indistinguishable between *Ddx46*$^{hi2137/+}$ and *Ddx46*$^{hi2137/hi2137}$ larvae at 48 hpf (Fig. II-8). It was very difficult to estimate cell proliferation of HSCs after 2.5 dpf because the EGFP fluorescence and the number of EGFP^{+} cells were profoundly reduced in *Ddx46*$^{hi2137/hi2137}$ larvae at these stages (Fig. II-9). These results indicate that the reduction of *tal1*-expressing HSCs in

Ddx46$^{hi2137/hi2137}$ larvae is not caused by the upregulation of cell death in the AGM and CHT or by the downregulation of cell proliferation of HSCs at 48 hpf.

Myelopoiesis occurs, but erythropoiesis and lymphopoiesis are suppressed in the CHT of *Ddx46*$^{hi2137/hi2137}$ mutants

An alternative possibility for the reduction of HSCs in *Ddx46*$^{hi2137/hi2137}$ larvae is that the multipotency of HSCs may be lost, and premature differentiation of HSCs to blood lineages may occur in *Ddx46*$^{hi2137/hi2137}$ mutants. To test this hypothesis, we examined the expression of various molecular markers for definitive hematopoiesis by whole-mount *in situ* hybridization. The expression of an erythroid marker *hemoglobin alpha embryonic-1* (*hbea1*) [32] was markedly reduced in *Ddx46*$^{hi2137/hi2137}$ mutants at 3 dpf (Fig. II-10A, B). We further found that the expression of lymphoid makers, *IKAROS family zinc finger 1* (*ikzf1*) [34] and *recombination activating gene 1* (*rag1*) [35], was lost in the thymus of *Ddx46*$^{hi2137/hi2137}$ mutants at 4 dpf (Fig. II-10C–F). However, the expression of *forkhead box N1* (*foxn1*) [36], a thymus epithelial marker, was indistinguishable between *Ddx46*$^{hi2137/+}$ and *Ddx46*$^{hi2137/hi2137}$ larvae (Fig. II-10G, H), indicating that thymus formation is normal in these mutants. Next, we tested the expression of myeloid markers such as *lymphocyte cytosolic plastin 1* (*lcp1*) [37] and mpx. In contrast to the erythroid and lymphoid markers, myeloid markers were not reduced in *Ddx46*$^{hi2137/hi2137}$ mutants at 3 dpf (Fig. II-10I–L). To exclude the possibility that the reduction of erythroid and lymphoid markers was not caused by the deficiency of Ddx46, we examined the results of the rescue experiments. We found that *hbea1* and *ikzf1* expression was partially rescued by *Ddx46* mRNA overexpression (Fig. II-11 and data not shown). Together, these results suggest that HSCs have defects in multi-lineage differentiation in *Ddx46*$^{hi2137/hi2137}$ mutants: they were able to differentiate to the myeloid fate, but differentiation to the erythroid or lymphoid fate was suppressed in the mutants.

Reduction of *gata1a* expression leads to erythropoiesis defects in *Ddx46*$^{hi2137/hi2137}$ mutants

Because recent articles have reported that the cross-antagonistic interactions between Gata1a and Spi1 transcription factors are critical for

deciding the differentiation to the erythroid or myeloid fate [2, 4, 5, 38], we examined the expression of these genes in *Ddx46*$^{hi2137/hi2137}$ mutants at 3 dpf (Fig. II-12A-E). Analyses of *in situ* hybridization and qPCR revealed that although *gata1a* expression was significantly reduced, *spi1* expression was maintained in the mutants (Fig. II-12A-E). To test whether the deficiency of erythropoiesis was caused by the reduction of *gata1a* in *Ddx46*$^{hi2137/hi2137}$ mutants, we carried out rescue experiments. Because phenotypic rescue of *vlad tepes* (*vlt*), a zebrafish *gata1a* mutant, was not achieved by overexpression of *gata1a* mRNA [39], we tried to use an efficient transient rescue method using the *Tol2* transposable element [29]. We found that the expression of an erythroid marker, *hbea1*, was partially rescued by this *Tol2*-mediated transgenesis method at 3 dpf (Fig. II-13). These results suggest that the suppression of erythropoiesis in *Ddx46*$^{hi2137/hi2137}$ mutants was due to the reduction of *gata1a* expression.

Ddx46$^{hi2137/hi2137}$ mutants have defects in pre-mRNA splicing in the hematopoietic cells

We previous elucidated that the unspliced mRNAs of *dla*, *her6*, *ptf1a*, and f*abp10a* were retained in the *Ddx46*$^{hi2137/hi2137}$ mutant. We further showed that the splicing of the housekeeping gene *actb1*, but not *b2m*, was normal in the heads of *Ddx46*$^{hi2137/hi2137}$ mutants. These results, combined with functional analyses of yeast Prp5 and human DDX46, suggest that zebrafish Ddx46 may be required for pre-mRNA splicing during development, and that the effect of splicing may be specific to a certain set of genes in the affected organs [20]. Hence, we examined the pre-mRNA splicing of *gata1a* and *spi1* by RT-PCR in this study. The RT-PCR analyses showed that although the unspliced mRNAs of *gata1a* were retained, the pre-mRNA splicing of *spi1* was normal in *Ddx46*$^{hi2137/hi2137}$ mutants at 3 dpf (Fig. II-12F-I). It is possible that the defects in pre-mRNA splicing lead to the reduction of *gata1a* expression and suppression of erythropoiesis in *Ddx46*$^{hi2137/hi2137}$ mutants. In addition to *gata1a* and *spi1*, we tested the pre-mRNA splicing of *cmyb* to examine the effect in HSCs. Similarly to *gata1a*; the unspliced mRNAs of *cmyb* were retained in *Ddx46*$^{hi2137/hi2137}$ mutants at 3 dpf (Fig. II-12J, K), suggesting that the defects in pre-mRNA splicing may affect the multi-lineage differentiation of HSCs (Fig. II-14).

Discussion

Status of HSCs in *Ddx46*$^{hi2137/hi2137}$ mutants

Although the expression of molecular markers for HSCs, such as *tal1*, *runx1*, or *cmyb*, was markedly reduced and proliferation of the HSCs was normal at 48 hpf, massive cell death of HSCs was not detected in *Ddx46*$^{hi2137/hi2137}$ mutants. There are several possibilities to explain the status of HSCs in *Ddx46*$^{hi2137/hi2137}$ mutants. One possible explanation is that, although the differentiation of HSCs is restricted to myeloid fate at the beginning of definitive hematopoiesis (around 30 hpf), the ability of differentiation to myeloid fate is lost at later stages, probably due to the reduction of *tal1*, *runx1*, and *cmyb* expressions in *Ddx46*$^{hi2137/hi2137}$ mutants at 3 dpf. Since previous studies have reported that Cmyb could regulate the expression of *tal1* and *runx1* in zebrafish and mouse HSCs, respectively [9,40], it is possible that splicing defects in *cmyb* result in the reduction of *tal1* and *runx1* expressions in HSCs of *Ddx46*$^{hi2137/hi2137}$ mutants. Another possibility is that HSCs continue to produce myeloid cells without the expressions of *tal1*, *runx1*, and *cmyb* during definitive hematopoiesis in *Ddx46*$^{hi2137/hi2137}$ mutants. Alternative possibility is that HSCs are lost, and they prematurely differentiate into myeloid cells. In both scenarios, the number of *lcp1* or *mpx* expressing myeloid cells should be increased in the mutants throughout definitive hematopoiesis. Since we have not analyzed the expression of molecular markers for myeloid cells at the beginning of definitive hematopoiesis, it is interesting to examine *spi1* expression in *Ddx46*$^{hi2137/hi2137}$ mutants at around 30 hpf. However, we showed that there was no striking difference in the number of myeloid cells between *Ddx46*$^{hi2137/+}$ and *Ddx46*$^{hi2137/hi2137}$ larvae at 3 dpf (Fig. II-10). Therefore, it is possible that the proliferation of the HSCs is reduced after 2.5 dpf. Unfortunately, due to the downregulation of EGFP fluorescence at 3 dpf, it was very difficult to evaluate the proliferation of HSCs using the Tg(*tal1*:*EGFP*) line (Fig. II-9). In contrast to *tal1*, the number of *cmyb*-expressing cells is higher than that of *tal1*-expressing cells during definitive hematopoiesis; this finding could be related to the fact that mouse *cmyb* is expressed in HSCs and progenitor cells [5]. In addition, *cmyb*

expressing cells are still present in *Ddx46*$^{hi2137/hi2137}$ mutants at 3 dpf (Fig. II-4G). Therefore, it may be important to analyze the cell proliferation after 2.5 dpf by using the *cmyb:EGFP* transgenic line. Currently, the presence of HSCs in *Ddx46*$^{hi2137/hi2137}$ mutants remains unknown because molecular markers of HSCs for maintenance and differentiation, except *tal1*, *runx1*, and *cmyb*, have not yet been reported in zebrafish. Further studies will therefore be necessary to identify the key target genes affected by the loss of *Ddx46* function for the maintenance and differentiation of HSCs.

Control of hematopoiesis by DExD/H-box RNA helicases

A recent report has revealed that Dhx8, a zebrafish orthologue of the yeast splicing factor Prp22, is involved in premRNA splicing and is required for primitive hematopoiesis [19]. In contrast to Prp5/Ddx46, the function of yeast Prp22 is critical for spliceosome disassembly when splicing reactions have been completed [16,17]. Although both *Ddx46* and *Dhx8* are maternal genes and are ubiquitously expressed during early somitogenesis, *Dhx8* mutants, but not *Ddx46*$^{hi2137/hi2137}$ mutants, showed defects in primitive hematopoiesis. One possible explanation for this phenotypic difference between *Ddx46*$^{hi2137/hi2137}$ and *Dhx8* mutants is that the function of Ddx46 is not necessary for primitive hematopoiesis and is specific for the control of HSC differentiation in zebrafish larvae. Alternatively, it is possible that because maternal transcripts of *Ddx46* or maternally derived Ddx46 proteins are more stable than those of Dhx8, defects in primitive hematopoiesis are rescued in *Ddx46*$^{hi2137/hi2137}$ mutants. Further studies will be needed to elucidate the detailed mechanisms that lead to hematopoiesis deficiencies and related diseases that are caused by DExD/H-box RNA helicases and/or splicing factors.

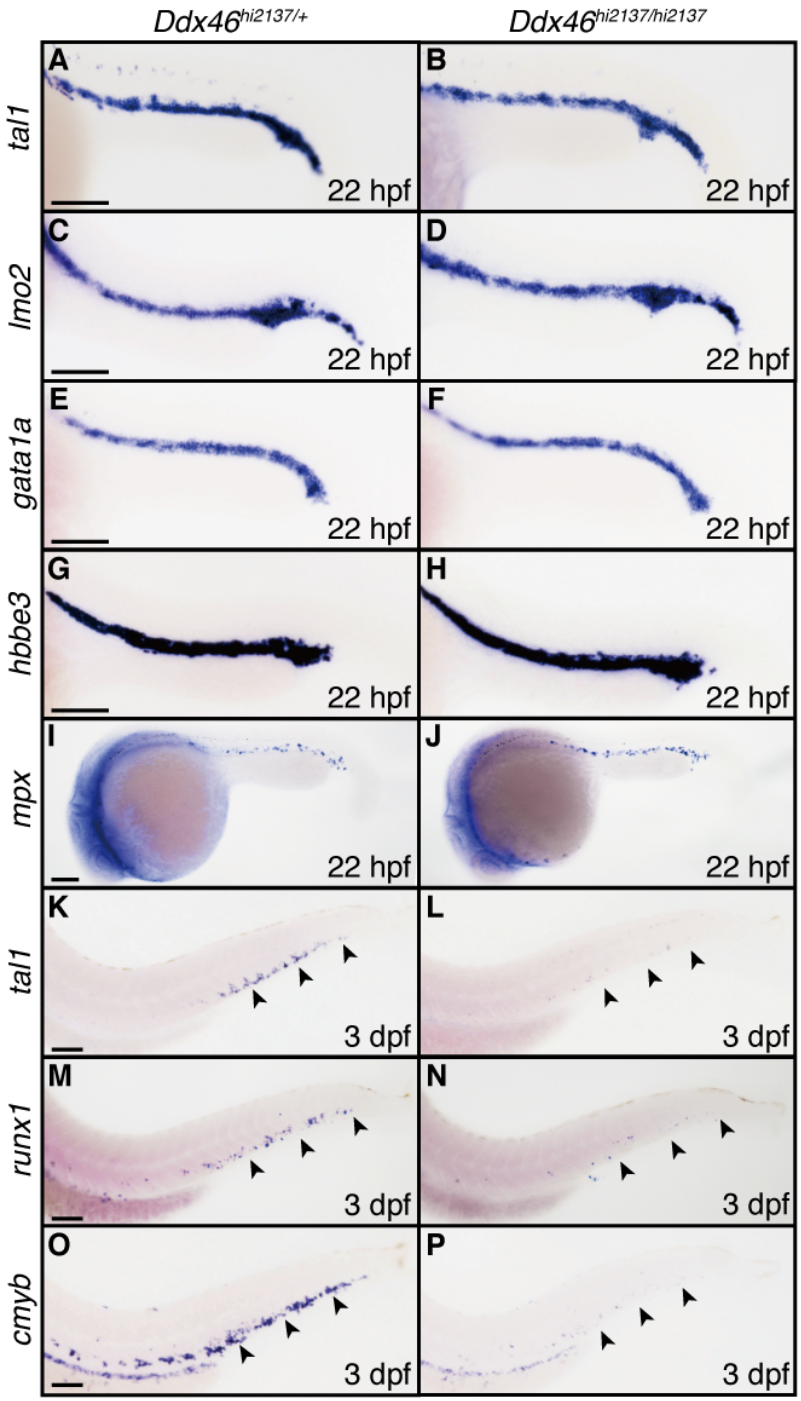

FIG. II-1. Definitive, but not primitive, hematopoiesis is defective in *Ddx46*$^{hi2137/hi2137}$ mutants.

(A–J) The expression of primitive hematopoietic markers, *tal1*, *lmo2*, *gata1a*, *hbbe3*, and *mpx*, and definitive hematopoietic markers, *tal1*, *runx1*, and *cmyb* was examined by whole-mount *in situ* hybridization at 22 hpf and 3 dpf, respectively. All are lateral views, anterior to the left. The expression of *tal1*, *lmo2*, *gata1a*, *hbbe3*, and *mpx* was

indistinguishable between *Ddx46*$^{hi2137/+}$ (*tal1*, n = 9/9; *lmo2*, n = 11/11; *gata1a*, n = 9/9; *hbbe3*, n = 12/12; *mpx*, n = 16/16) and *Ddx46*$^{hi2137/hi2137}$ embryos (*tal1*, n = 9/9; *lmo*2, n = 9/9; *gata1a*, n = 7/7; *hbbe3*, n = 10/10; *mpx*, n = 7/7) at 22 hpf (A–J). In contrast, the number of cells expressing *tal1*, *runx1*, and *cmyb* in *Ddx46*$^{hi2137/hi2137}$ larvae (*tal1*, n = 6/6; *runx1*, n = 9/9; *cmyb,* n = 11/11) was markedly reduced compared with that in *Ddx46*$^{hi2137/+}$ larvae (*tal1*, n = 8/8; *runx1*, n = 11/11; *cmyb*, n = 13/13) at 3 dpf (arrowheads in K– P).

Scale bars represent 100 mm. *tal1, T-cell acute lymphocytic leukemia 1*; *lmo2*, *LIM domain only 2*; *gata1a, GATA-binding protein 1a; hbbe3*, *hemoglobin beta embryonic-3*; *mpx*, *myeloid specific peroxidase*; *runx1, Runt-related transcription factor 1.*

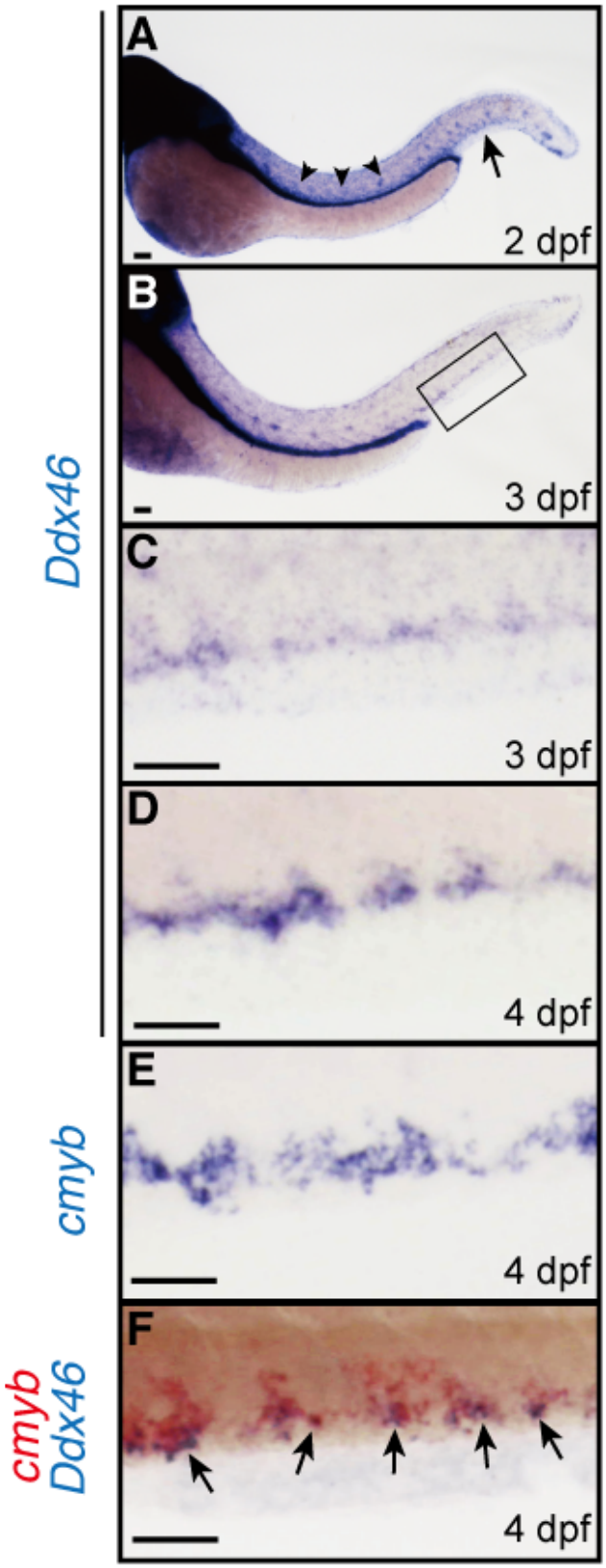

FIG. II-2. *Ddx46* expression in HSCs.

The expression of *Ddx46* and *cmyb* in wild-type larvae was examined by whole-mount *in situ* hybridization at 2, 3, and 4 dpf. All are lateral views, anterior to the left. (A-C) *Ddx46* is ubiquitously expressed in the AGM (arrowheads in A) and CHT (arrow in A) at 2 dpf (n=6/6) and is specifically expressed in the CHT (boxed area in B) at 3 dpf (n=6/6). The boxed area in (B) is shown enlarged in (C).

(D, E) The transcripts of both genes (*Ddx46*, n=11/11; *cmyb*, n=9/9) were detected in the CHT at 4 dpf. (F) Double whole-mount *in situ* staining showed that the expression domains of *Ddx46* (blue) and *cmyb* (red) overlapped in the CHT (arrows) (n=7/7) at 4 dpf.

Scale bars represent 50mm.

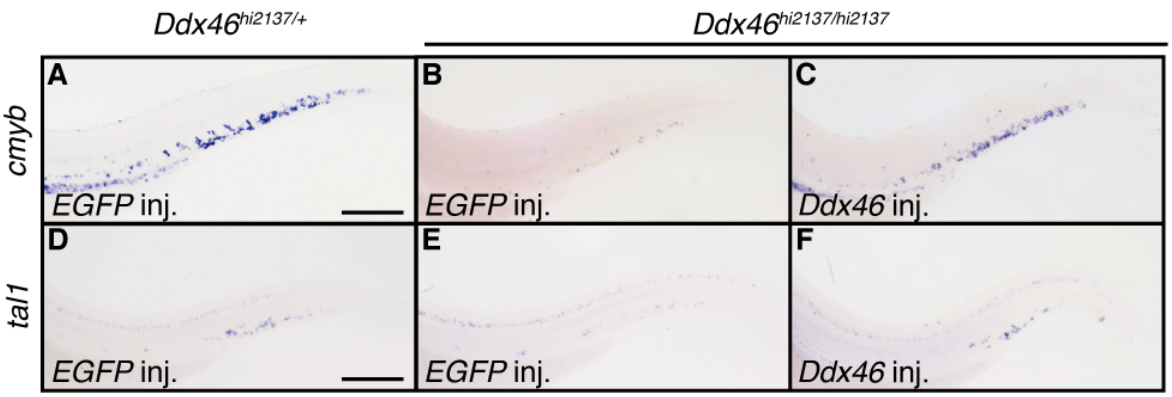

FIG. II-3. Expression of *cmyb* and *tal1* in *Ddx46*$^{hi2137/hi2137}$ mutants is rescued by over expression of *Ddx46* mRNA.

(A–F) The expression of *cmyb* and *tal1* was examined by whole-mount *in situ* hybridization at 3 dpf. All are lateral views, anterior to the left. The number of *cmyb*- or *tal1*-expressing HSCs in the *EGFP* mRNA-injected *Ddx46*$^{hi2137/hi2137}$ larvae (*cmyb*, 0 of 26 *EGFP* mRNA-injected mutants were rescued; tal1, 0 of 21 *EGFP* mRNA-injected mutants were rescued) was markedly lower than that in the *EGFP* mRNA-injected *Ddx46*$^{hi2137/+}$ larvae (*cmyb*, n = 17/17; *tal1*, n = 16/16) at 3 dpf (A, B, D, E). The over expression of *Ddx46* mRNA was able to rescue the number of *cmyb*- or *tal1*-expressing HSCs in *Ddx46*$^{hi2137/hi2137}$ larvae (*cmyb*, 19 of 21 *Ddx46* mRNA-injected mutants were rescued; *tal1*, 19 of 22 *Ddx46* mRNA-injected mutants were rescued) at 3 dpf (B, C, E, F). Scale bars represent 100 mm.

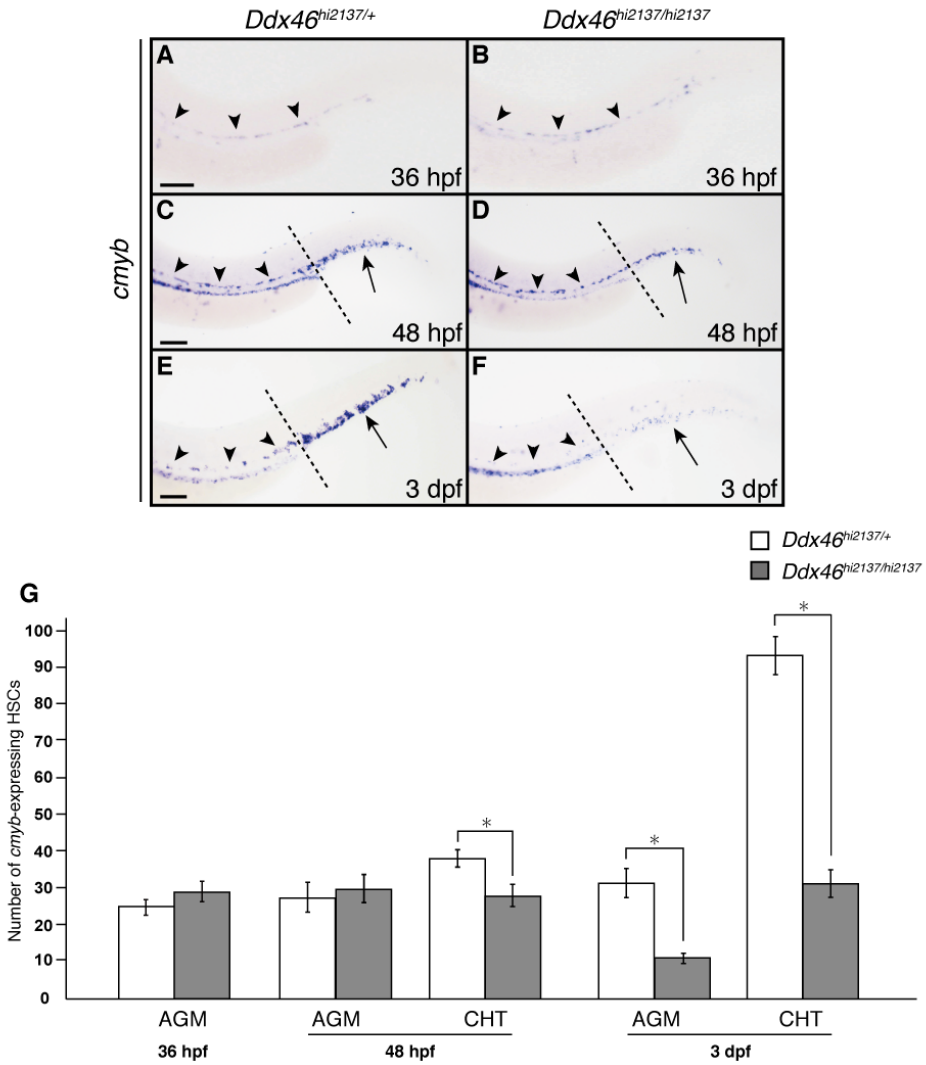

FIG. II-4. Number of *cmyb*-expressing cells decreases in *Ddx46*$^{hi2137/hi2137}$ mutants.

(A–G) The expression of *cmyb* was examined by whole-mount *in situ* hybridization at 36hpf, 48 hpf, or 3 dpf. All are lateral views, anterior to the left. The number of *cmyb*-expressing HSCs in the AGM (arrowheads) and CHT (arrows) was counted at 36 hpf, 48hpf, and 3 dpf (G). At 36 hpf, the number of *cmyb*-expressing HSCs in the AGM (arrowheads) was indistinguishable between *Ddx46*$^{hi2137/+}$and *Ddx46*$^{hi2137/hi2137}$ larvae (A, B, G). In contrast, the number of *cmyb* expressing HSCs in the CHT (arrows), but not in the AGM (arrowheads), at 48 hpf (C, D, G) and in both the AGM (arrowheads) and CHT (arrows) at 3 dpf (E, F, G) of *Ddx46*$^{hi2137/hi2137}$ larvae was significantly reduced compared with that of *Ddx46*$^{hi2137/+}$ larvae. *Ddx46*$^{hi2137/+}$ larvae: n = 13/13 (36 hpf), n = 18/18 (48 hpf), n = 13/13 (3 dpf); *Ddx46*$^{hi2137/hi2137}$larvae: n = 9/9 (36hpf), n = 14/14 (48 hpf), n = 11/11 (3dpf). Black dotted lines in (C–F) indicate the boundary between the AGM and CHT. Error bars represent the standard error. *$P < 0.01$ by the Student's *t*-test. Scale bars represent100 mm.

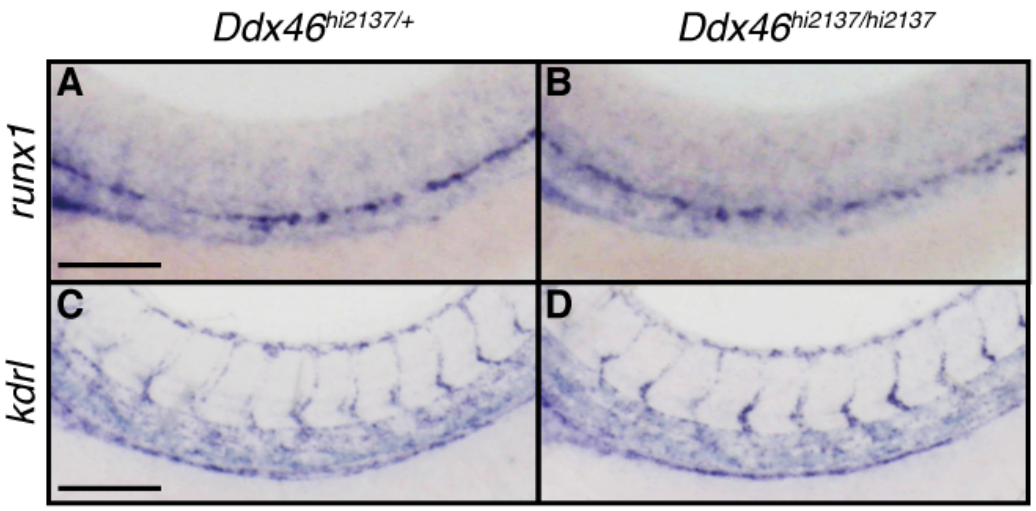

FIG. II-5. Expression of *runx1* and *kdrl* is normal in *Ddx46*$^{hi2137/hi2137}$ mutants.

(A–D) The expression of *runx1* and *kdrl* was examined by whole-mount *in situ* hybridization at 48 hpf. All are lateral views, anterior to the left. The expression of *runx1* and *kdrl* was indistinguishable between *Ddx46*$^{hi2137/+}$ (*runx1*, n = 25/25; *kdrl*, n = 7/7) and *Ddx46*$^{hi2137/hi2137}$ larvae (*runx1*, n = 13/13; *kdrl*, n = 7/7). Scale bars represent 100 mm.

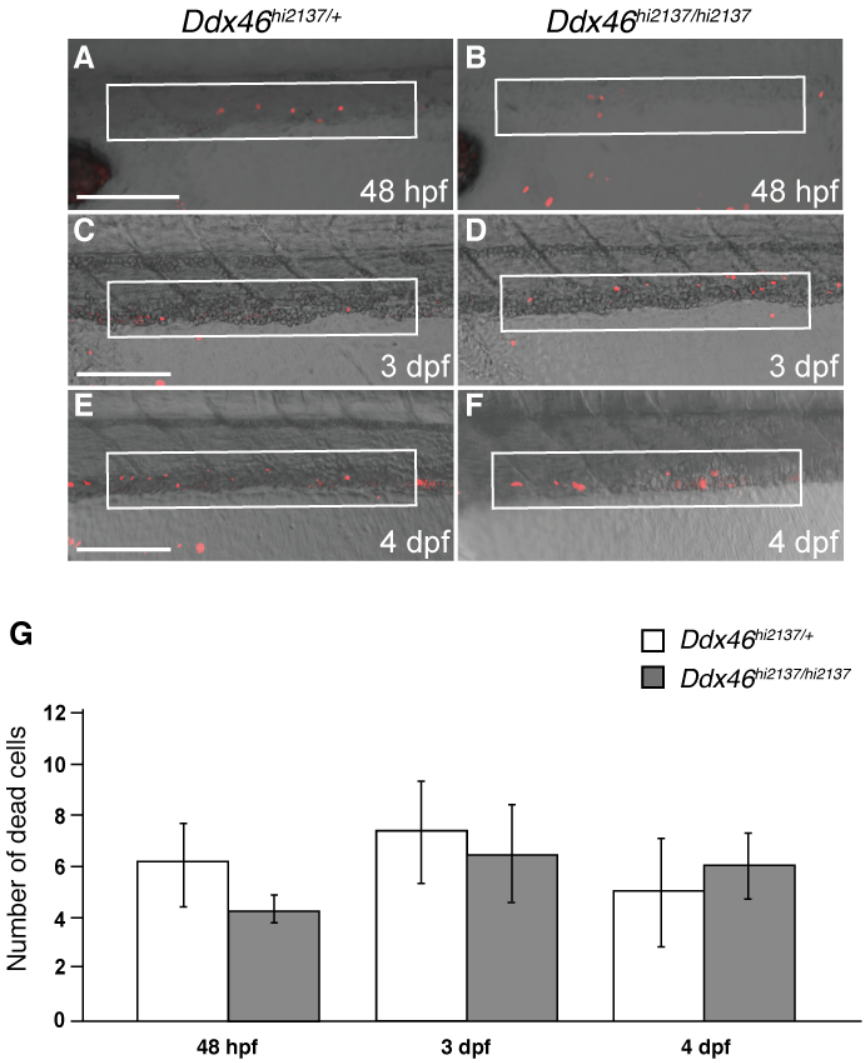

FIG. II-6. Cell death is not up regulated in the CHT of *Ddx46*$^{hi2137/hi2137}$ mutants.

(A–F) Confocal microscopic images of dead cells (red) detected by the TUNEL method at 48 hpf, 3 dpf, or 4 dpf. All are lateral views, anterior to the left. The white, boxed regions show an area of the CHT. (G) The number of labeled cells in the white, boxed regions (A–F) was counted. The number of dead cells in the CHT was indistinguishable between *Ddx46*$^{hi2137/+}$and *Ddx46*$^{hi2137/hi2137}$ larvae at48 hpf, 3 dpf, and 4 dpf. *Ddx46*$^{hi2137/+}$ larvae: n = 7/7(48 hpf), n = 5/5 (3 dpf), n = 5/5 (4 dpf); *Ddx46*$^{hi2137/hi2137}$larvae: n = 5/5 (48 hpf), n = 6/6 (3 dpf), n = 8/8 (4dpf). Error bars represent the standard error. Scale bars represent 75 mm.

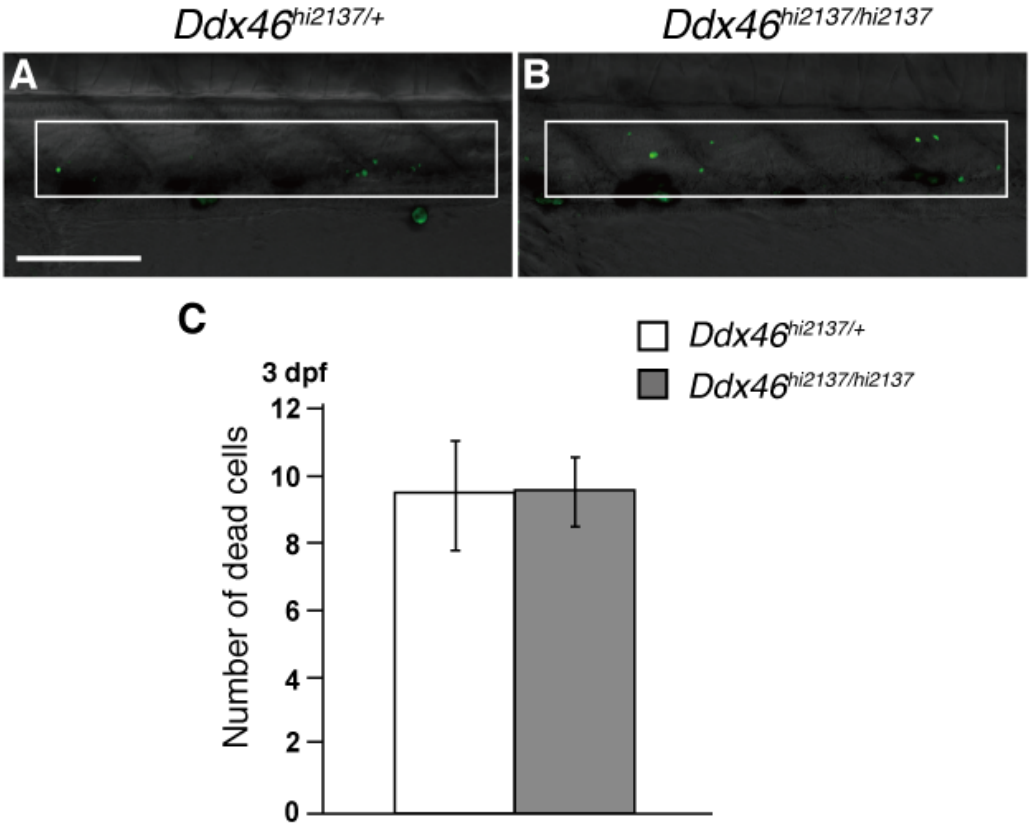

FIG. II-7. Upregulation of cell death is not detected in the CHT of *Ddx46*$^{hi2137/hi2137}$ mutants.

(A, B) Confocal microscopic images of dead cells (green) detected by acridine orange staining at 3 dpf. All are lateral views, anterior to the left. The white, boxed regions show an area of the CHT. (C) The number of dead cells in *Ddx46*$^{hi2137/hi2137}$ larvae (n = 6/6) was not higher than in *Ddx46*$^{hi2137/+}$ larvae (n = 5/5). Error bars represent the standard error. The scale bar represents 75 mm.

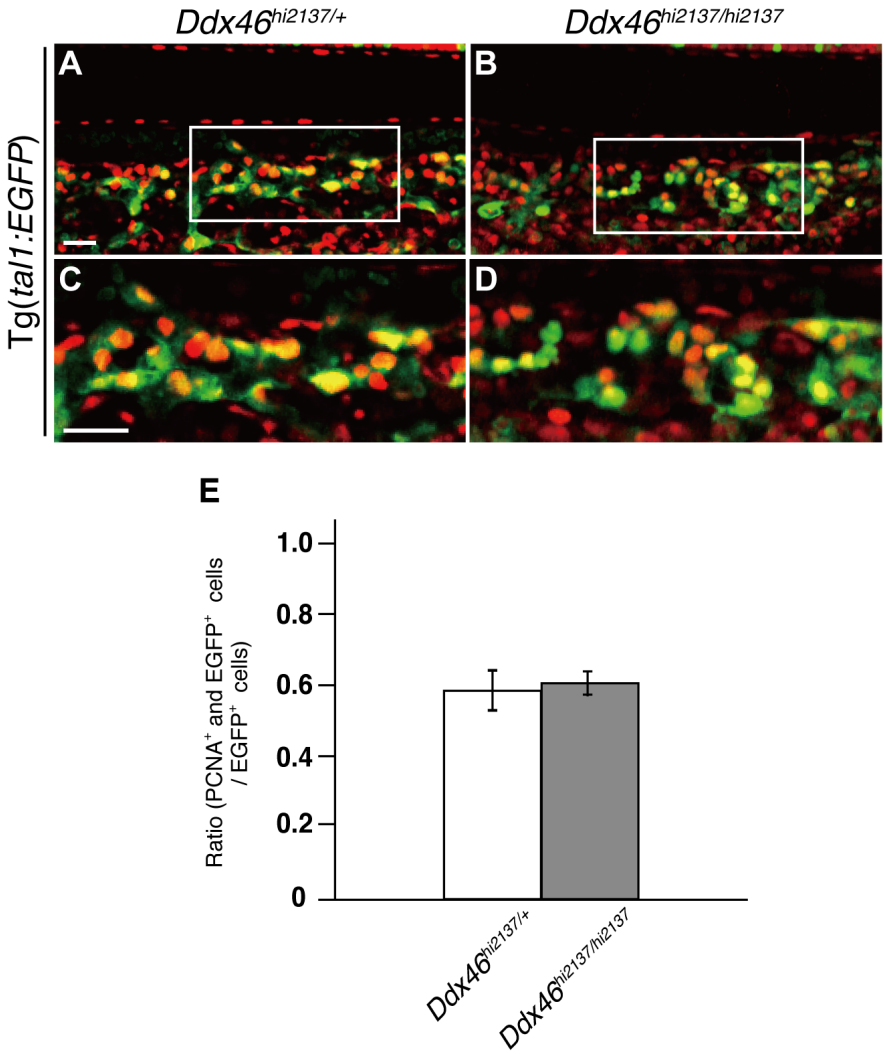

FIG. II-8. Cell proliferation is not down regulated in the CHT of *Ddx46*$^{hi2137/hi2137}$ mutants at 48 hpf.

(A–D) Confocal microscopic images of EGFP fluorescence (green) and anti-PCNA (red) whole-mount immunostaining of the CHT in *Ddx46*$^{hi2137/+}$; Tg(*tal1:EGFP*) and *Ddx46*$^{hi2137/hi2137}$; Tg(*tal1:EGFP*) larvae at 48 hpf. All are lateral views, anterior to the left. Merged single slice images of cells expressing EGFP (HSCs) and PCNA (proliferating cells). The boxed areas in (A) and (B) are shown enlarged in (C) and (D), respectively. (E) Quantification of the experiments in panels(C) and (D) was performed by plotting the ratio of EGFP$^+$ and PCNA$^+$ cells (yellow) to the total number of EGFP$^+$ cells (green and yellow). No significant difference between *Ddx46*$^{hi2137/+}$; Tg(*tal1:EGFP*) and *Ddx46*$^{hi2137/hi2137}$; Tg(*tal1:EGFP*) larvae was observed. Cells were counted from four single slices from four embryos for each condition. Error bars represent the standard error. The scale bar represents 20 mm. PCNA, proliferating cell nuclear antigen.

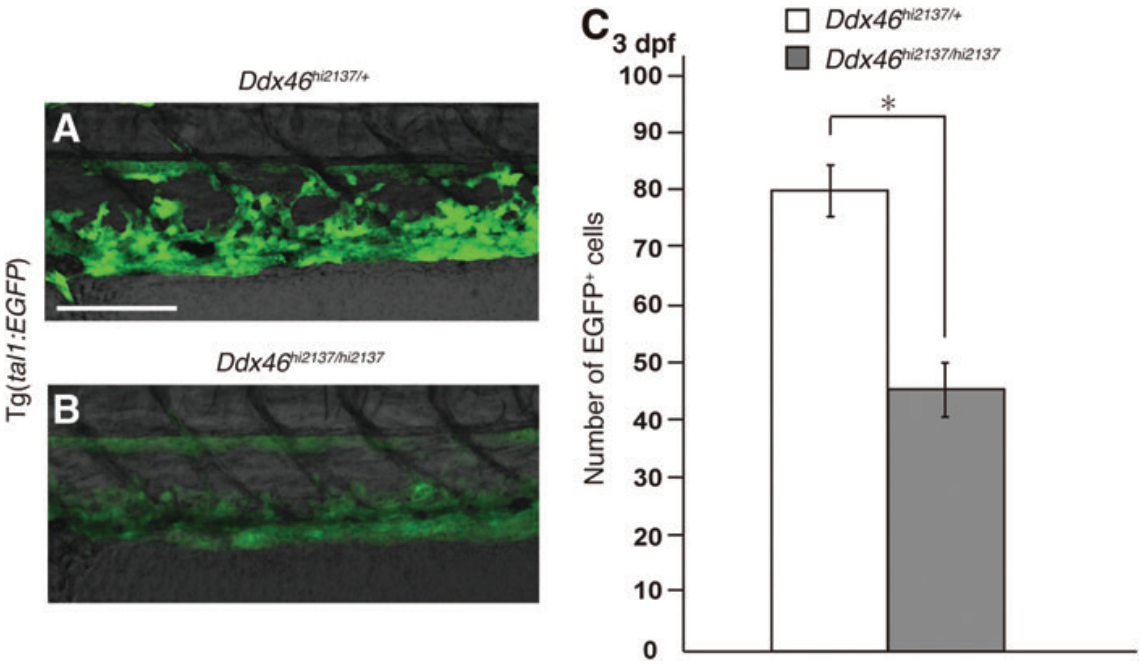

FIG. II-9. Expression of the *tal1:EGFP* transgene is markedly reduced in *Ddx46*$^{hi2137/hi2137}$; Tg(*tal1:EGFP*) larvae.

(A, B) Confocal microscopic images of EGFP fluorescence (green) of the CHT in *Ddx46*$^{hi2137/+}$; Tg(*tal1:EGFP*) and *Ddx46*$^{hi2137/hi2137}$; Tg(*tal1:EGFP*) larvae at 3 dpf. All are lateral views, anterior to the left. (C) The number of EGFP^{+} cells in *Ddx46*$^{hi2137/hi2137}$; Tg(*tal1:EGFP*) larvae (n = 6/6) was significantly reduced compared with that in *Ddx46*$^{hi2137/+}$; Tg(*tal1:EGFP*) larvae (n = 5/5). *$P < 0.01$ by the Student's *t*-test. Error bars represent the standard error. The scale bar represents 75 mm.

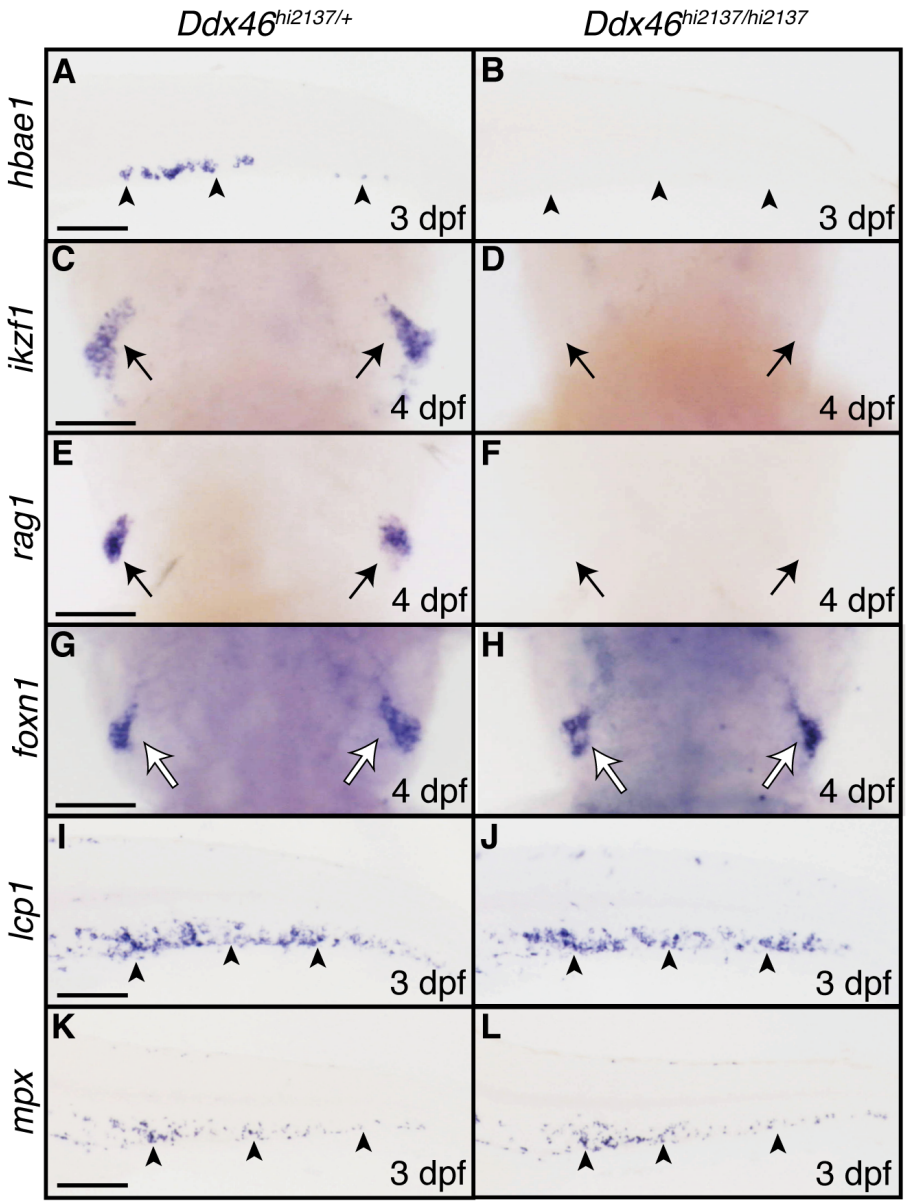

FIG. II-10. Myelopoiesis occurs, but erythropoiesis and lymphopoiesis are suppressed in *Ddx46*$^{hi2137/hi2137}$ mutants.

(A–L) The expression of molecular markers for erythrocytes, lymphocytes, myelocytes, and a thymus epithelium was examined by whole-mount *in situ* hybridization at 3 and 4 dpf. Lateral views, anterior to the left (A, B, I–L). Dorsal views, anterior to the top (C–H). The expression of a definitive erythroid marker *hbae1* was markedly reduced in *Ddx46*$^{hi2137/hi2137}$ larvae at 3 dpf (arrowheads in A, B) (*Ddx46*$^{hi2137/hi2137}$larvae, n = 7/7; *Ddx46*$^{hi2137/+}$ larvae, n = 9/9). The expression of lymphoid markers, ikzf1 (*Ddx46*$^{hi2137/hi2137}$ larvae, n = 9/9;*Ddx46*$^{hi2137/+}$ larvae, n = 9/9) and *rag1* (*Ddx46*$^{hi2137/hi2137}$ larvae, n = 9/9; *Ddx46*$^{hi2137/+}$ larvae, n = 7/7), was lost in*Ddx46*$^{hi2137/hi2137}$ larvae (black arrows in C–F),

whereas the expression of a thymus epithelial marker *foxn1* was indistinguishable between *Ddx46*$^{hi2137/+}$ (n = 7/7) and *Ddx46*$^{hi2137/hi2137}$ larvae (n = 9/9) at 4 dpf (white arrows in G, H). In contrast, the expression of myeloid markers, *lcp1* (*Ddx46*$^{hi2137/hi2137}$ larvae, n = 8/8; *Ddx46*$^{hi2137/+}$ larvae, n = 8/8) and mpx (*Ddx46*$^{hi2137/hi2137}$ larvae, n = 12/13; *Ddx46*$^{hi2137/+}$ larvae, n = 8/8), was maintained in *Ddx46*$^{hi2137/hi2137}$ larvae at3 dpf (arrowheads in I–L). Scale bars represent 100 mm. *hbae1*, *hemoglobin alpha embryonic-1*; *ikzf1*, *IKAROS family zincfinger 1*; *rag1*, *recombination activating gene 1*; *foxn1*, *forkhead box N1*; *lcp1*, *lymphocyte cytosolic plastin 1*.

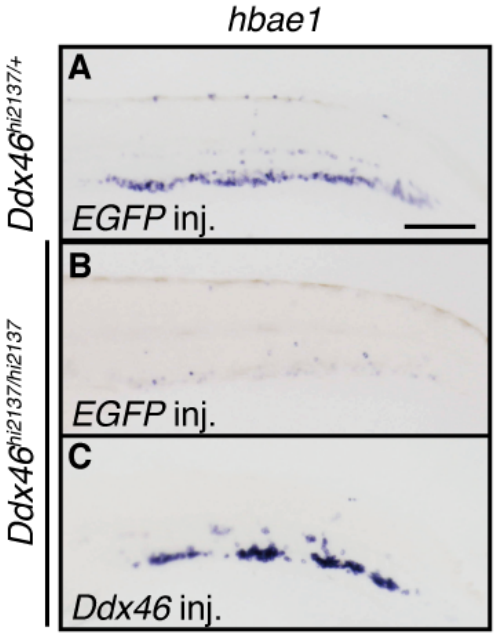

FIG. II-11. Expression of *hbae1* in *Ddx46*$^{hi2137/hi2137}$ mutants is rescued by *Ddx46* mRNA overexpression.

(A–C) The expression of *hbae1* was examined by whole-mount *in situ* hybridization at 3 dpf. All are lateral views, anterior to the left. The expression of *hbae1* in the *EGFP* mRNA-injected *Ddx46*$^{hi2137/hi2137}$ larvae (n = 14/14) was markedly lower than that in the *EGFP* mRNA-injected *Ddx46*$^{hi2137/+}$ larvae (n = 9/9) at 3 dpf (A, B). The expression of *hbae1* in *Ddx46*$^{hi2137/hi2137}$ larvae was rescued by *Ddx46* mRNA overexpression at 3 dpf (13 of 13 *Ddx46* mRNA-injected mutants were rescued) (B, C). The scale bar represents 100 mm.

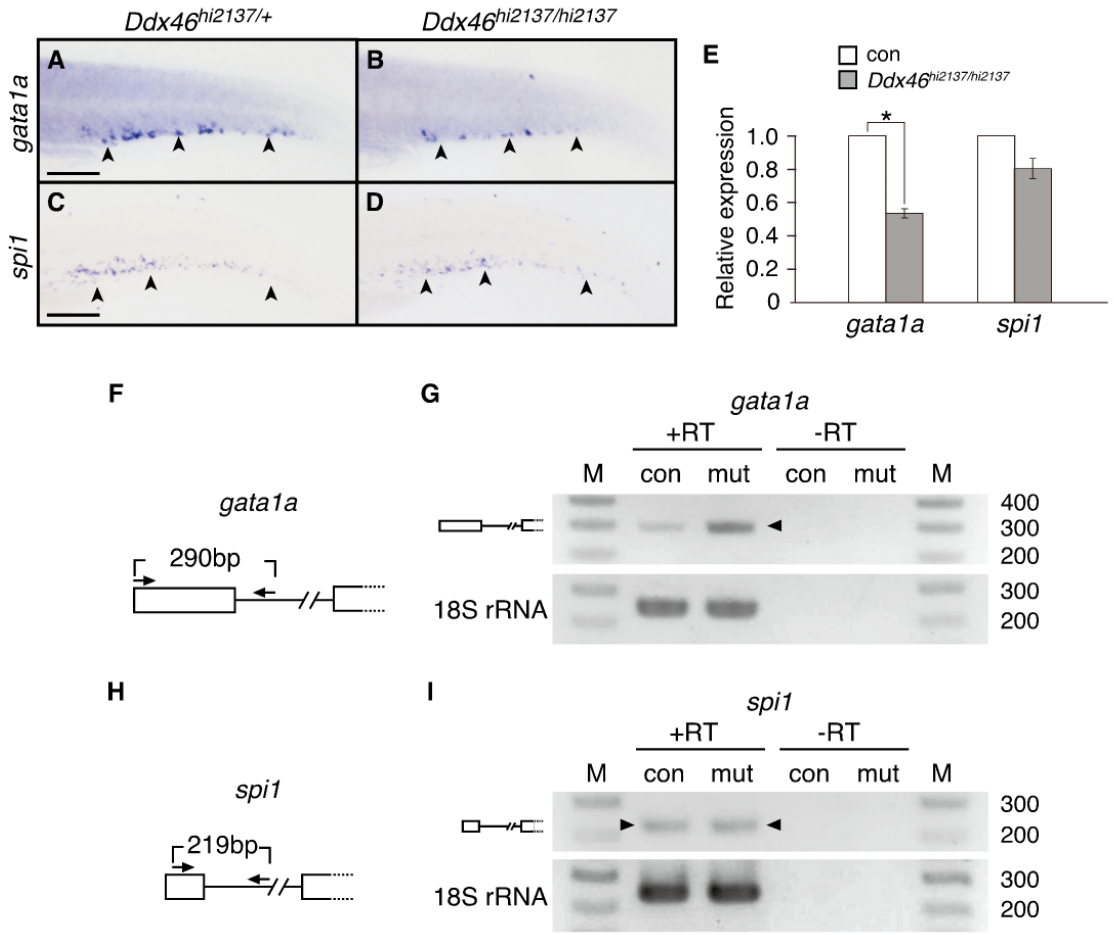

FIG. II-12. Expression and pre-mRNA splicing of gata1a, but not *spi1*, are defective in *Ddx46*$^{hi2137/hi2137}$ mutants.

(A–D) The expression of *gata1a* and *spi1* was examined by whole-mount *in situ* hybridization at 3 dpf. All are lateral views, anterior to the left. The expression of *gata1a* in the CHT of *Ddx46*$^{hi2137/hi2137}$ larvae (n = 10/10) was markedly reduced compared with that of *Ddx46*$^{hi2137/+}$ larvae (n = 10/10) (arrowheads in A, B). In contrast, *spi1* expression in the CHT of *Ddx46*$^{hi2137/hi2137}$ larvae (n = 10/10) was maintained compared with that of *Ddx46*$^{hi2137/+}$ larvae (n = 9/9) (arrowheads in C, D). Scale bars represent100 mm. (E) Relative expression of *gata1a* and *spi1* genes in control (con) larvae compared with that in *Ddx46*$^{hi2137/hi2137}$ larvae at 3 dpf, by qPCR. Although no significant difference of *spi1* expression was found between con and *Ddx46*$^{hi2137/hi2137}$ larvae, *gata1a* expression in *Ddx46*$^{hi2137/hi2137}$larvae was significantly lower than that in con larvae. *$P < 0.01$ by the Student's t-test. Error bars represent the standard error. (F–K) Schematic drawings of the *gata1a*, *spi1*, and *cmyb* pre-mRNA regions analyzed for splicing (boxes, exons; lines, introns; arrows, primers) (F, H, J). The splicing status of *gata1a*, *spi1*, or *cmyb* pre-mRNA was monitored by RT-PCR with the primers indicated in schemes (F),

(H), or (J), respectively. The reverse primer for *gata1a* or *spi1*m RNA was designed within the intron (F, H). The forward primer for *cmyb* crosses the exon14/intron14 boundary (J). Unspliced gata1a or *cmyb* mRNA was retained at a higher level in *Ddx46*$^{hi2137/hi2137}$ mutant (mut) larvae than in con larvae (arrowhead in G= 290 bp; arrowhead in K= 156 bp). In contrast, the level of unspliced *spi1* mRNA was indistinguishable between the mut larvae and con larvae (arrowheads in I = 219 bp). Unspliced PCR products were verified by sequencing. +RT refers to the validation reaction itself, and -RT represents the respective control reaction without reverse transcriptase. 18SrRNA is a loading control. Control larvae were sibling WT or *Ddx46*$^{hi2137/+}$ larvae, and they had normal phenotypes. qPCR, quantitative polymerase chain reaction; RT, reverse transcription.

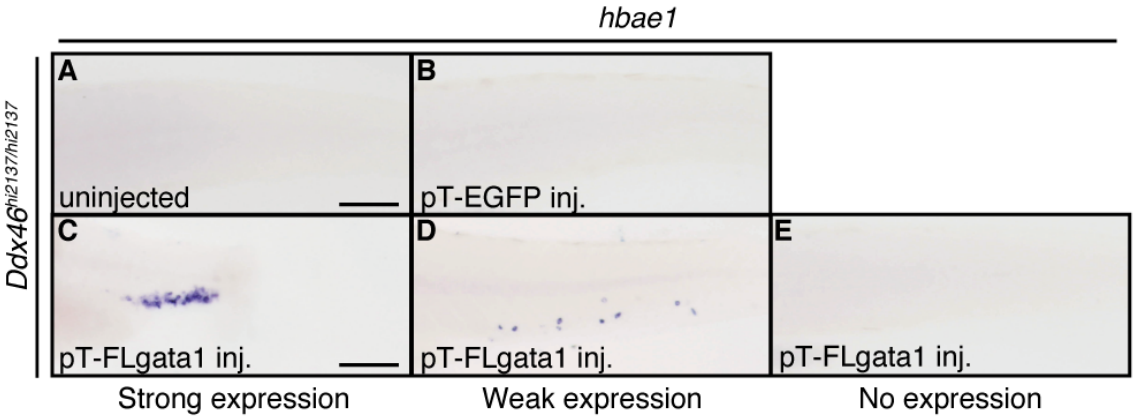

FIG. II-13. Expression of hbae1 in *Ddx46*$^{hi2137/hi2137}$ mutants is rescued by the *Tol2-gata1a* vector.

(A–E) The expression of *hbae1* was examined by whole-mount *in situ* hybridization at 3 dpf. All are lateral views, anterior to the left. (A, B) No staining of *hbae1* was observed in uninjected *Ddx46*$^{hi2137/hi2137}$ mutants (n = 7/7). The *hbae1* expression was not rescued by exogenous *EGFP* expression by using pT-*EGFP* in *Ddx46*$^{hi2137/hi2137}$ mutants (0 of 21 pT-EGFP + *Tol2-transposase* mRNA-injected mutants were rescued). (C–E) On the other hand, the *hbae1* expression was partially rescued by exogenous *gata1a* expression using pT-FLgata1 in *Ddx46*$^{hi2137/hi2137}$ mutants (strong *hbae1* expression, 6 of 39 pT-FLgata1 + *Tol2-transposase* mRNA-injected mutants were rescued; weak *hbae1* expression, 10 of 39 pT-FLgata1 + *Tol2-transposase* mRNA-injected mutants were rescued; no *hbae1* expression, 23 of 39 pT-FLgata1 + *Tol2-transposase* mRNA-injected mutants were not rescued). Scale bars represent 100 mm.

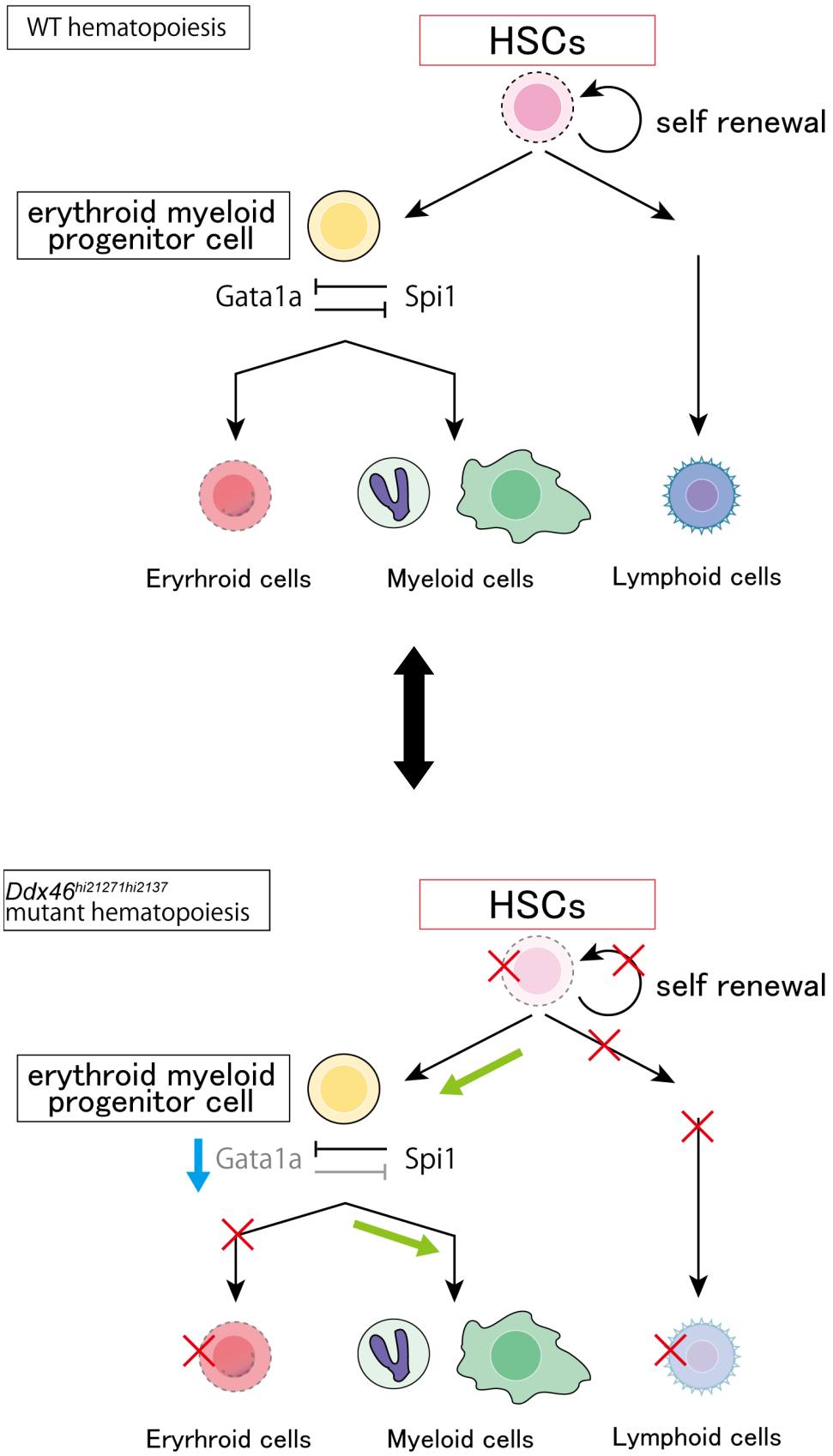
WT hematopoiesis
HSCs
self renewal
erythroid myeloid progenitor cell
Gata1a
Spi1
Eryrhroid cells
Myeloid cells
Lymphoid cells
Ddx46hi21271hi2137 mutant hematopoiesis
HSCs
self renewal
erythroid myeloid progenitor cell
Gata1a
Spi1
Eryrhroid cells
Myeloid cells
Lymphoid cells

FIG. II-14. The model of hematopoiesis in WT and *Ddx46*$^{hi2137/hi2137}$ mutants.

These models explain wild type and *Ddx46*$^{hi2137/2137}$ mutant blood cell differentiation in definitive hematopoiesis. The *Ddx46*$^{hi2137/2137}$ mutant model is based on our results of the Ddx46 study. HSCs markers were reduced in *Ddx46*$^{hi2137/2137}$ mutants, but HSCs differentiation in AGM is normal at 48 hpf. These results suggest that HSCs lost the function of maintenance and self-renewal. Our analysis of blood lineage marker expression revealed that each erythropoiesis and lymphopoiesis is suppressed in *Ddx46*$^{hi2137/2137}$ mutant, but myelopoiesis was normally. The expression of *gata1a* was markedly reduced, but not *spi1* in *Ddx46*$^{hi2137/2137}$ mutants.

TABLE II-1. The list and sequence of primers used for RT-PCR analysis

Primer	Sequence
gata1a exon2 forward	ATGGAGAACTCCTCTGAGCC
gata1a intron2 reverse	GTGCATGTCTTCAGACAGCTTC
spi1 exon3 forward	GATCTATCGACCACCAATGGAG
spi1 intron3 reverse	GAGCAGCAGTAGAGTCTGTTC
cmyb intron14 forward	CACGACATGCCTGTGAGTATC
cmyb exon15 reverse	TGTGTCCGTCCTCAGTCTTC
18S rRNA forward	CCGCTAGAGGTGAAATTCTTG
18S rRNA reverse	CAGCTTTGCAACCATACTCC

TABLE II-2. PCR thermal cycler program for RT-PCR

Genes	Initial denaturation	Denaturation	Annealing	Elongation	Final elongation	Cycling No.
gata1a *exon2-intron2*	95 °C, 2 min	95 °C, 30 sec	63 °C, 30 sec	72 °C, 30sec	-----	35
spi1 *exon3-intron3*	95 °C, 2 min	95 °C, 30 sec	60.2 °C, 30 sec	72 °C, 30sec	72 °C, 7 min	35
cmyb *intron14-exon15*	95 °C, 2 min	95 °C, 30 sec	63 °C, 30 sec	72 °C, 30sec	-----	37
18S rRNA	95 °C, 2 min	95 °C, 30 sec	60 °C, 30 sec	72 °C, 30sec	72 °C, 7 min	26

References

1. Cumano A and I Godin. (2007). Ontogeny of the hematopoietic system. Annu Rev Immunol 25:745-85.

2. Orkin SH and LI Zon. (2008). Hematopoiesis: an evolving paradigm for stem cell biology. Cell 132:631-44.

3. Medvinsky A, S Rybtsov and S Taoudi. (2011). Embryonic origin of the adult hematopoietic system: advances and questions. Development 138:1017-31.

4. Carradice D and GJ Lieschke. (2008). Zebrafish in hematology: sushi or science? Blood 111:3331-42.

5. Paik EJ and LI Zon. (2010). Hematopoietic development in the zebrafish. Int J Dev Biol 54:1127-37.

6. Mucenski ML, K McLain, AB Kier, SH Swerdlow, CM Schreiner, TA Miller, DW Pietryga, WJ Scott and SS Potter. (1991). A functional c-myb gene is required for normal murine fetal hepatic hematopoiesis. Cell 65:677-89.

7. Sumner R, A Crawford, M Mucenski and J Frampton. (2000). Initiation of adult myelopoiesis can occur in the absence of c-Myb whereas subsequent development is strictly dependent on the transcription factor. Oncogene 19:3335-42.

8. Lieu YK and EP Reddy. (2009). Conditional c-myb knockout in adult hematopoietic stem cells leads to loss of self-renewal due to impaired proliferation and accelerated differentiation. Proc Natl Acad Sci U S A 106:21689-94.

9. Soza-Ried C, I Hess, N Netuschil, M Schorpp and T Boehm. (2010). Essential role of c-myb in definitive hematopoiesis is evolutionarily conserved. Proc Natl Acad Sci U S A 107:17304-8.

10. Zhang Y, H Jin, L Li, FX Qin and Z Wen. (2011). cMyb regulates hematopoietic stem/progenitor cell mobilization during zebrafish hematopoiesis. Blood 118:4093-101.

11. North TE, MF de Bruijn, T Stacy, L Talebian, E Lind, C Robin, M Binder, E Dzierzak and NA Speck. (2002). Runx1 expression marks long-term repopulating hematopoietic stem cells in the midgestation mouse embryo. Immunity 16:661-72.

12. Burns CE, T DeBlasio, Y Zhou, J Zhang, L Zon and SD Nimer. (2002). Isolation and characterization of runxa and runxb, zebrafish members of the runt family of transcriptional regulators. Exp Hematol 30:1381-9.

13. Chen MJ, T Yokomizo, BM Zeigler, E Dzierzak and NA Speck. (2009). Runx1 is required for the endothelial to haematopoietic cell transition but not thereafter. Nature 457:887-91.

14. Sood R, MA English, CL Belele, H Jin, K Bishop, R Haskins, MC McKinney, J Chahal, BM Weinstein, Z Wen and PP Liu. (2010). Development of multilineage adult hematopoiesis in the zebrafish with a runx1 truncation mutation. Blood 115:2806-9.

15. Lancrin C, P Sroczynska, C Stephenson, T Allen, V Kouskoff and G Lacaud. (2009). The haemangioblast generates haematopoietic cells through a haemogenic endothelium stage. Nature 457:892-5.

16. Rocak S and P Linder. (2004). DEAD-box proteins: the driving forces behind RNA metabolism. Nat Rev Mol Cell Biol 5:232-41.

17. Bleichert F and SJ Baserga. (2007). The long unwinding road of RNA helicases. Mol Cell 27:339-52.

18. Payne EM, N Bolli, J Rhodes, OI Abdel-Wahab, R Levine, CV Hedvat, R Stone, A Khanna-Gupta, H Sun, JP Kanki, HT Gazda, AH Beggs, FE Cotter and AT Look. (2011). Ddx18 is essential for cell-cycle progression in zebrafish hematopoietic cells and is mutated in human AML. Blood 118:903-15.

19. English MA, L Lei, T Blake, SM Wincovitch, R Sood, M Azuma, D Hickstein and PP Liu. (2012). Incomplete splicing, cell division defects, and hematopoietic blockage in dhx8 mutant zebrafish. Dev Dyn 241:879-89.

20. Hozumi S, R Hirabayashi, A Yoshizawa, M Ogata, T Ishitani, M Tsutsumi, A Kuroiwa, M Itoh and Y Kikuchi. (2012). DEAD-box protein Ddx46 is required for the development of the digestive organs and brain in zebrafish. PLoS One 7:e33675.

21. Westerfield M. (1993). The zebrafish book A guide for the laboratory use of zebrafish Danio (Brachydanio) rerio. Institute of Neuroscience, University of Oregon,, Eugene, OR.

22. Kimmel CB, WW Ballard, SR Kimmel, B Ullmann and TF Schilling. (1995). Stages of embryonic development of the zebrafish. Dev Dyn 203:253-310.

23. Amsterdam A, RM Nissen, Z Sun, EC Swindell, S Farrington and N Hopkins. (2004). Identification of 315 genes essential for early zebrafish development. Proc Natl Acad Sci U S A 101:12792-7.

24. Gering M, AR Rodaway, B Göttgens, RK Patient and AR Green. (1998). The SCL gene specifies haemangioblast development from early mesoderm. EMBO J 17:4029-45.

25. Zhang XY and AR Rodaway. (2007). SCL-GFP transgenic zebrafish: in vivo imaging of blood and endothelial development and identification of the initial site of definitive hematopoiesis. Dev Biol 307:179-94.

26. Urasaki A, G Morvan and K Kawakami. (2006). Functional dissection of the Tol2 transposable element identified the minimal cis-sequence and a highly repetitive sequence in the subterminal region essential for transposition. Genetics 174:639-49.

27. Mizoguchi T, H Verkade, JK Heath, A Kuroiwa and Y Kikuchi. (2008). Sdf1/Cxcr4 signaling controls the dorsal migration of endodermal cells during zebrafish gastrulation. Development 135:2521-9.

28. Detrich HW, MW Kieran, FY Chan, LM Barone, K Yee, JA Rundstadler, S Pratt, D Ransom and LI Zon. (1995). Intraembryonic hematopoietic cell migration during vertebrate development. Proc Natl Acad Sci U S A 92:10713-7.

29. Takeuchi M, H Kaneko, K Nishikawa, K Kawakami, M Yamamoto and M Kobayashi. (2010). Efficient transient rescue of hematopoietic mutant phenotypes in zebrafish using Tol2-mediated transgenesis. Dev Growth Differ 52:245-50.

30. Lieschke GJ, AC Oates, BH Paw, MA Thompson, NE Hall, AC Ward, RK Ho, LI Zon and JE Layton. (2002). Zebrafish SPI-1 (PU.1) marks a site of myeloid development independent of primitive erythropoiesis: implications for axial patterning. Dev Biol 246:274-95.

31. Thompson MA, DG Ransom, SJ Pratt, H MacLennan, MW Kieran, HW Detrich, B Vail, TL Huber, B Paw, AJ Brownlie, AC Oates, A Fritz, MA Gates, A Amores, N Bahary, WS Talbot, H Her, DR Beier, JH Postlethwait and LI Zon. (1998). The cloche and spadetail genes differentially affect hematopoiesis and vasculogenesis. Dev Biol 197:248-69.

32. Brownlie A, C Hersey, AC Oates, BH Paw, AM Falick, HE Witkowska, J Flint, D Higgs, J Jessen, N Bahary, H Zhu, S Lin and L Zon. (2003). Characterization of embryonic globin genes of the zebrafish. Dev Biol 255:48-61.

33. Bennett CM, JP Kanki, J Rhodes, TX Liu, BH Paw, MW Kieran, DM Langenau, A Delahaye-Brown, LI Zon, MD Fleming and AT Look. (2001). Myelopoiesis in the zebrafish, Danio rerio. Blood 98:643-51.

34. Willett CE, H Kawasaki, CT Amemiya, S Lin and LA Steiner. (2001). Ikaros expression as a marker for lymphoid progenitors during zebrafish development. Dev Dyn 222:694-8.

35. Willett CE, AG Zapata, N Hopkins and LA Steiner. (1997). Expression of zebrafish rag genes during early development identifies the thymus. Dev Biol 182:331-41.

36. Schorpp M, M Leicht, E Nold, M Hammerschmidt, A Haas-Assenbaum, W Wiest and T Boehm. (2002). A zebrafish orthologue (whnb) of the mouse nude gene is expressed in the epithelial compartment of the embryonic thymic rudiment. Mech Dev 118:179-85.

37. Herbomel P, B Thisse and C Thisse. (1999). Ontogeny and behaviour of early macrophages in the zebrafish embryo. Development 126:3735-45.

38. Monteiro R, C Pouget and R Patient. (2011). The gata1/pu.1 lineage fate paradigm varies between blood populations and is modulated by tif1γ. EMBO J 30:1093-103.

39. Lyons SE, ND Lawson, L Lei, PE Bennett, BM Weinstein and PP Liu. (2002). A nonsense mutation in zebrafish gata1 causes the bloodless phenotype in vlad tepes. Proc Natl Acad Sci U S A 99:5454-9.

40. Dai G, H Sakamoto, Y Shimoda, T Fujimoto, S Nishikawa and M Ogawa. (2006). Over-expression of c-Myb increases the frequency of hemogenic precursors in the endothelial cell population. Genes Cells 11:859-70.

IV. General Discussion

Ddx46 function in zebrafish

Our studies of the zebrafish Ddx46 function revealed novel Ddx46 function *in vivo*. In zebrafish, loss of Ddx46 is the fatal damage to embryogenesis, and our previous visual phenotypic analysis found defects in digestive organs and brain [1]. In this study, we also found HSCs defects in the term of definitive hematopoiesis by gene expression analysis. Through the both previous and this hematopoietic study, we found that specific pre-mRNA splicing is responsible for these defects and it controls the tissue and organ formation.

Ddx46 mutants show defects in the digestive organs and brain, and massive cell apoptosis is found in these defects sites. In contrast, *Ddx46* mutants also show the defects in definitive hematopoiesis but massive cell apoptosis cannot be identified in hematopoietic defects. We, therefore, expect that the distinction of apoptotic cells between the defects in both digestive organs and brain and definitive hematopoiesis in *Ddx46* mutants also depend on the gene specificity of pre-mRNA splicing mediated by Ddx46. Some apoptosis related genes could be activated in digestive organs and brain when specific gene pre-mRNA splicing defects goes on.

Specific pre-mRNA splicing mediated by Ddx46

When people hear and think about the specific pre-mRNA splicing or selectivity of splicing, many people will be able to come up with alternative splicing first. Certainly, alternative splicing could be known for the specific pre-mRNA splicing. It produces different mature mRNA translated as splicing variants by changing combination of exons [2]. Alternative splicing is the mechanism to making various proteins from one of genes and it regulates gene expression [2]. The report showed that alternative splicing regulates gene expression during terminal erythropoiesis [3]. In contrast, the specificity of pre-mRNA splicing mediated by Ddx46 means genes selection in general pre-mRNA splicing, and pre-mRNA retained in *Ddx46* mutant would be degraded or translated into non-functional proteins. Therefore, Ddx46 affects the accuracy of pre-mRNA splicing and controls gene expression, but doesn't have the function to make various proteins.

Splicing is an essential process during gene expression and producing

protein, but our study found that pre-mRNA splicing mediated by Ddx46 has the specificity for gene selection. According to previous studies, each Prp5 and Ddx46 is involved in major splicing process by associated with U1 and U2 snRNP [4-7]. Then our study shows that pre-mRNA splicing is the essential process but pre-mRNA splicing mediated Ddx46 is not involved in all genes splicing.

Roles of pre-mRNA splicing factors in hematopoiesis

Because pre-mRNA splicing of *gata1a* and *cmyb*, but not *spi1*, is defective in *Ddx46*$^{hi2137/hi2137}$ mutants (Fig. II-12), it is possible that aberrant pre-mRNAs lead to reduced *gata1a* and *cmyb* expressions. Our results suggest that pre-mRNA splicing is associated with hematopoiesis in zebrafish. Recently, numerous studies using whole-exome sequencing revealed that recurrent mutations in spliceosome subunits have been implicated in hematopoietic malignancies [8-11]. The 4 genes encoding spliceosome components, *U2 small nuclear RNA auxiliary factor 1* (*U2AF1*; also known as *U2AF35*), *splicing factor 3B subunit 1* (*SF3B1*), *U2AF1-related protein* (*ZRSR2*; also known as *Urp*), and *serine/arginine rich splicing factor 2* (*SRSF2*), are frequently mutated in chronic lymphocytic leukemia (CLL) and/or myelodysplastic syndrome (MDS) [8-11]. It is well known that these 4 components are involved in the initial steps of pre-mRNA splicing for the establishment of spliceosome complexes E and A: U2AF1 and SRSF2 bind to the 3' splice acceptor site of the pre-mRNA: ZRSR2 interacts with U2AF1 and a serine/ arginine-rich SR protein: and SF3B1, which is a component of the U2 small nuclear ribonucleoprotein (U2snRNP), binds to the branch point sequence of the pre-mRNA [12,13]. These results suggest that the initial steps of pre-mRNA splicing are closely related to hematopoietic malignancies in mammals. Yeast DExD/H-box proteins, Sub2, Prp5, Prp28, Brr2, Prp2, Prp16, Prp22, and Prp43, act in specific steps of the splicing cycles to catalyze RNA–RNA rearrangements and RNP remodeling [14, 15]. Among these, it has been determined that Saccharomyces cerevisiae Prp5 (a yeast orthologue of vertebrate Ddx46) and human DDX46 are able to interact with U2snRNP [14-16]. These reports, combined with the splicing factor studies in hematopoietic malignancies, suggest that the 4 splicing components (U2AF1, SF3B1, ZRSR2, and SRSF2) and Ddx46 play critical roles in the initial steps of pre-mRNA splicing, and these factors may

function in the maintenance and/or differentiation of HSCs. Although recurrent mutations in DDX46 have not yet been reported in patients with CLL and/or MDS by whole-exome sequencing, it is possible that mutations in DDX46 cause hematopoietic malignancies.

A relationship between specific pre-mRNA splicing and prespliceosome formation

Recent study reported *U2AF1* mutation alters the splicing site recognition in hematological malignancies and the specificity of pre-mRNA binding and splicing [17, 18]. This *U2AF1* mutation site is immediately upstream of the 3' splice acceptor site [18]. In addition, most recent study revealed the novel Prp5 function in the pre-mRNA splicing. Previous studies revealed Prp5 is required for the formation of prespliceosome through the ATP-dependent U2 remodeling [8-12], but Prp5 also has the function of proofreading the branch site sequence in association with U2 [19]. Prp5 directly binds to U2 branchpoint-interaction stem-loops (BSL), and kept correctly pre-mRNA splicing. Prp5 mutant suppressed BSL binding, showed retain of the pre-mRNA by splicing defects [19]. In this report, the pre-mRNA splicing defects depending on suppression of BSL binding is independent of ATPase activity. However, our previous study and another study for Prp5 found ATPase domain is required for pre-mRNA splicing [1, 20]. In contrast both two reports even said importance of association between Prp5 and U2 [19, 20]. These results suggest that Ddx46 has two different functions in pre-mRNA splicing and both functions affect the pre-mRNA splicing mediated by associating with U2. Then, prespliceosome formation mediated by U2 may decide the specificity of gene in pre-mRNA splicing.

Finally we found specificity of pre-mRNA splicing and it controls tissue and organ formation. These validations and results, however, have not revealed the mechanism of pre-mRNA splicing clearly and specific target for Ddx46.

Therefore, we have to explore the specific target gene to reveal the mechanism of tissue and organ formation controlled by Ddx46.

References

1. Hozumi S, R Hirabayashi, A Yoshizawa, M Ogata, T Ishitani, M Tsutsumi, A Kuroiwa, M Itoh and Y Kikuchi. (2012). DEAD-box protein Ddx46 is required for the development of the digestive organs and brain in zebrafish. PLoS One 7:e33675.

2. Smith CW, JG Patton and B Nadal-Ginard. (1989). Alternative splicing in the control of gene expression. Annu Rev Genet 23:527-77.

3. Pimentel H, M Parra, S Gee, D Ghanem, X An, J Li, N Mohandas, L Pachter and JG Conboy. (2014). A dynamic alternative splicing program regulates gene expression during terminal erythropoiesis. Nucleic Acids Res 42:4031-42.

4. Ruby SW, Chang TH, Abelson J (1993) Four yeast spliceosomal proteins (PRP5, PRP9, PRP11, and PRP21) interact to promote U2 snRNP binding to premRNA. Genes Dev 7: 1909–1925.

5. Xu Y, Newnham C, Kameoka S, Huang T, Konarska M, et al. (2004) Prp5 bridges U1 and U2 snRNPs and enables stable U2 snRNP association with intron RNA. EMBO J 23: 376–385.

6. Xu YZ, Query CC (2007) Competition between the ATPase Prp5 and branch region-U2 snRNA pairing modulates the fidelity of spliceosome assembly. Mol Cell 28: 838–849.

7. Kosowski TR, HR Keys, TK Quan and SW Ruby. (2009). DExD/H-box Prp5 protein is in the spliceosome during most of the splicing cycle. RNA 15:1345-62.

8. Yoshida K, M Sanada, Y Shiraishi, D Nowak, Y Nagata, R Yamamoto, Y Sato, A Sato-Otsubo, A Kon, M Nagasaki, G Chalkidis, Y Suzuki, M Shiosaka, R Kawahata, T Yamaguchi, M Otsu, N Obara, M Sakata-Yanagimoto, K Ishiyama, H Mori, F Nolte, WK Hofmann, S Miyawaki, S Sugano, C Haferlach, HP Koeffler, LY Shih, T Haferlach,

S Chiba, H Nakauchi, S Miyano and S Ogawa. (2011). Frequent pathway mutations of splicing machinery in myelodysplasia. Nature 478:64-9.

9. Hahn CN and HS Scott. (2012). Spliceosome mutations in hematopoietic malignancies. Nat Genet 44:9-10.

10. Quesada V, L Conde, N Villamor, GR Ordóñez, P Jares, L Bassaganyas, AJ Ramsay, S Beà, M Pinyol, A Martínez-Trillos, M López-Guerra, D Colomer, A Navarro, T Baumann, M Aymerich, M Rozman, J Delgado, E Giné, JM Hernández, M González-Díaz, DA Puente, G Velasco, JM Freije, JM Tubío, R Royo, JL Gelpí, M Orozco, DG Pisano, J Zamora, M Vázquez, A Valencia, H Himmelbauer, M Bayés, S Heath, M Gut, I Gut, X Estivill, A López-Guillermo, XS Puente, E Campo and C López-Otín. (2012). Exome sequencing identifies recurrent mutations of the splicing factor SF3B1 gene in chronic lymphocytic leukemia. Nat Genet 44:47-52.

11. Graubert TA, D Shen, L Ding, T Okeyo-Owuor, CL Lunn, J Shao, K Krysiak, CC Harris, DC Koboldt, DE Larson, MD McLellan, DJ Dooling, RM Abbott, RS Fulton, H Schmidt, J Kalicki-Veizer, M O'Laughlin, M Grillot, J Baty, S Heath, JL Frater, T Nasim, DC Link, MH Tomasson, P Westervelt, JF DiPersio, ER Mardis, TJ Ley, RK Wilson and MJ Walter. (2012). Recurrent mutations in the U2AF1 splicing factor in myelodysplastic syndromes. Nat Genet 44:53-7.

12. Tronchère H, J Wang and XD Fu. (1997). A protein related to splicing factor U2AF35 that interacts with U2AF65 and SR proteins in splicing of pre-mRNA. Nature 388:397-400.

13. Wahl MC, CL Will and R Lührmann. (2009). The spliceosome: design principles of a dynamic RNP machine. Cell 136:701-18.

14. Rocak S, Linder P (2004) DEAD-box proteins: the driving forces behind RNA metabolism. Nat Rev Mol Cell Biol 5: 232–241.

15. Bleichert F, Baserga S (2007) The long unwinding road of RNA helicases. Mol Cell 27:339–352.

16. Xu YZ, CM Newnham, S Kameoka, T Huang, MM Konarska and CC Query. (2004). Prp5 bridges U1 and U2 snRNPs and enables stable U2 snRNP association with intron RNA. EMBO J 23:376-85.

17. Ilagan JO, A Ramakrishnan, B Hayes, ME Murphy, AS Zebari, P Bradley and RK Bradley. (2015). U2AF1 mutations alter splice site recognition in hematological malignancies. Genome Res 25:14-26.

18. Okeyo-Owuor T, BS White, R Chatrikhi, DR Mohan, S Kim, M Griffith, L Ding, S Ketkar-Kulkarni, J Hundal, KM Laird, CL Kielkopf, TJ Ley, MJ Walter and TA Graubert. (2014). U2AF1 mutations alter sequence specificity of pre-mRNA binding and splicing. Leukemia.

19. Liang WW and SC Cheng. (2015). A novel mechanism for Prp5 function in prespliceosome formation and proofreading the branch site sequence. Genes Dev 29:81-93.

20. Zhang ZM, F Yang, J Zhang, Q Tang, J Li, J Gu, J Zhou and YZ Xu. (2013). Crystal structure of Prp5p reveals interdomain interactions that impact spliceosome assembly. Cell Rep 5:1269-78.

Acknowledgment

This study carried out in Laboratory of Developmental Biology, Department of Biological science, Graduate School of science, Hiroshima University.

I express my sincere thanks to professor Y. Kikuchi, assistant professor S Hozmumi, Hiroshima University, for their invaluable advice, discussion and tutelage throughout course of this study. We also thank Drs. Atsuo Kawahara and Makoto Kobayashi for providing DNA templates; and Dr Atushi Szuki, all member of Atushi Suzuki laboratory for helpful discussion and critical comments. This work was supported by a grant from the Sasakawa Foundation.

Finally Thanks to my family and all member of Kikuchi laboratory for their advice and encouragement.

公表論文

Publication

Ddx46 is required for multi-lineage differentiation of hematopoietic stem cells in zebrafish.
Ryo hirabayashi, Shunya Hozumi, Shin-ichi Higashijima, and Yutaka Kikuchi
Stem cells and Development 2013 sep. 22 (18) pp. 2532-2542